



INDIAN INSTITUTE OF TECHNOLOGY KANPUR

NACDeC-VI: The Design Challenge 2022 - Air Ambulance



TASK-I REPORT

Faculty Advisor

Prof.Mangal Kothari | Aerospace Engineering | mangal@iitk.ac.in

Authors

Vardhaman Jain | Aerospace Engineering

Aaryansh Mohan Bansal | Aerospace Engineering

Lavanya Ingle | Aerospace Engineering

Dikhith Pragada | Aerospace Engineeirng

Tushar Kumar | Mechanical Engineering

Contents

1	Background	4
1.1	Configuration selection	4
2	Mission Specifications	4
3	Methodology	5
4	Sizing	7
5	Weight Estimation	7
5.1	Empirical Method	7
5.2	Statistical Method	9
5.3	Conclusion	10
6	Wing Design	11
6.1	Multi-Mode Constraints Analysis (MCA)	11
6.1.1	Hovering Flight	12
6.1.2	Vertical Climb Flight/Takeoff	12
6.1.3	Stall Speed	13
6.1.4	Maximum Forward Speed	13
6.1.5	Rate of Climb	14
6.2	New Proposed Method	16
6.2.1	Background	17
6.3	Methodology	19
6.4	Airfoil Selection	25
6.5	3D Wing Design	26
7	Tail Design	27
8	Rotor Selection and Performance	31
9	Powertrain Design	33
9.1	Introduction	33
9.2	Types of Hybrid Systems[9]	34

9.3	Which Hybrid System to choose?	35
9.4	Design[8]	35
9.5	Motor Sizing[8]	36
9.6	Cell Selection	37
9.6.1	Sample Calculation	38
9.6.2	Result[4]	39
9.7	Fuel Cell as a Secondary source of energy![5]	40
9.7.1	Fuel Cell Design	40
9.8	Volume occupied by Battery set and Fuel cell	41
9.8.1	Battery	41
9.8.2	Fuel Cell[7]	42
10	Fuselage Design	42
10.1	Introduction	42
10.2	Dimensions	43
10.3	Ergonomics	43
10.4	Cabin Design	43
10.5	Outer Skin Design	45
10.5.1	Iterations	45
10.6	Accommodation of Cabin in the Fuselage	46
10.7	CFD Analysis	46

1 Background

1.1 Configuration selection

This section consists of the technical details followed from the previous report(Synopsis report) on the basis of which the present report has been developed. In the earlier report, we have shown the choice of our design drivers and accordingly the importance assigned to these design drivers relative to each other. The Pugh matrix was derived based on the calculation of the weights done by the standard procedure.

We then carried out a detailed literature review on the possible configurations possible for EV-TOL. The primary focus was on the variation of design drivers among these configurations. Based on the study the AHP matrix was obtained which helped us in choosing the ideal configuration for our Air Ambulance design.1 shows our derived AHP matrix.

Prioritization Matrix	Safety	Speed	Acoustics	Maintainability & Reliability	Size	Hover Efficiency	Payload Fraction	Maneuverability	Ease of Certification	Transition	Cost
Safety	1	2	4	9	3	9	8	9	6	5	7
Speed	1/2	1	3	8	2	9	7	9	5	4	6
Acoustics	1/4	1/3	1	6	1/2	8	5	7	3	2	4
Maintainability & Reliability	1/9	1/8	1/6	1	1/7	3	1/2	2	1/4	1/5	1/3
Size	1/3	1/2	2	7	1	9	6	8	4	3	5
Hover Efficiency	1/9	1/9	1/8	1/3	1/9	1	1/4	1/2	1/6	1/4	1/5
Payload fraction	1/8	1/7	1/5	2	1/6	4	1	3	1/3	1/2	1/4
Maneuverability	1/9	1/9	1/7	1/2	1/8	2	1/3	1	1/5	1/6	1/4
Ease of Certification	1/6	1/5	1/3	4	1/4	6	3	5	1	0.500	2.000
Transition	1/5	1/4	1/2	5	1/3	4	2	6	2	1.000	3.000
Cost	1/7	1/6	1/4	3	1/5	5	4	4	1/2	1/3	1.000
Column Sum	3.051	4.940	11.718	45.833	7.829	60.000	37.083	54.500	22.450	16.950	29.033

Figure 1: AHP Matrix for our design

The top three configurations were Lift+Cruise, Tilt ducted fans with fixed wings, and multi-copter. However, as mentioned in a former report the Tilt ducted fans with fixed wings had to be eliminated primarily due to the lack of open-source technology available in that domain. This design gained second preference in AHP matrix due to the optimal design of Lilium Jet. But practically it would be difficult since the technology which makes the Lilium jet favorable will not be easy to develop at this level. Therefore Multicopter and Lift+Cruise designs were studied in detail. Finally, after a detailed trade-off study of multicopter and lift+cruise configuration, we **finalized Lift+Cruise as our configuration for Air Ambulance.**

2 Mission Specifications

Our aim is the conceptual design of an urban-friendly fully autonomous EVTOL air ambulance. While some of the parameters like medical payload are common and inherently known, other specifications like human payload, range, endurance, speed, etc. have to be provided by

the customer or the user. The problem statement of the competition has provided the following mission profile for Task-I and some of the mission specification parameters. The 2 below and the values in 1 have been directly taken from the official problem statement.

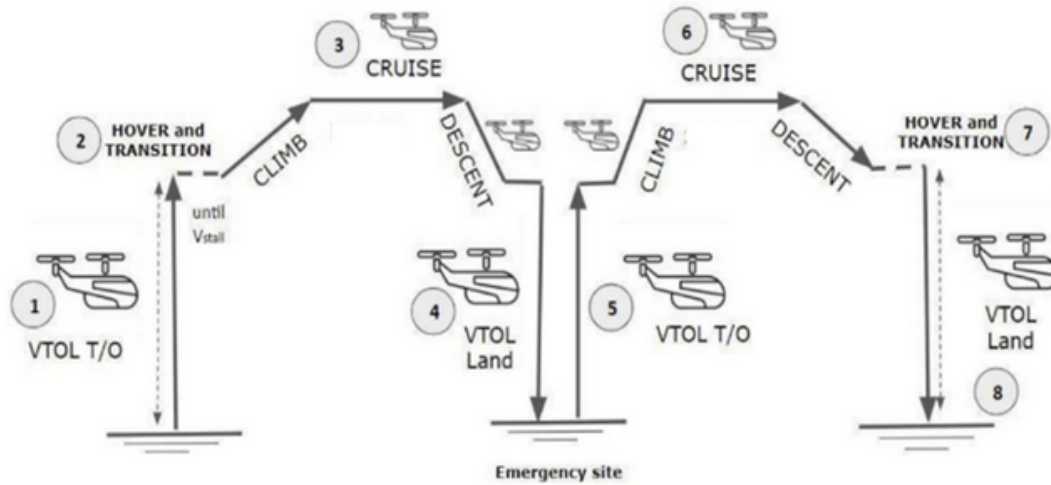


Figure 2: Mission Profile

Mission Specifications	
Variable	Values
Mass of Patient and paramedic	170kg
Range	100km
Cruise Speed	120km/h
Pax Cabin Volume	$9.0m^3$
Pax Cabin Dimensions	$3.0m \times 2.0m \times 1.5m$

Table 1: Mission Specification given by the problem statement

Other mission specification parameters like stall speed, maximum speed, service ceiling, absolute ceiling, etc. have not been specified in the problem statement. Therefore it becomes important for us to properly decide and perform trade-off studies on the possible values of these parameters, since these would bring upon the blueprint of the conceptual design of our vehicle.

3 Methodology

There have been numerous literary articles, research papers, authentic books and online courses on the design methodology for fixed-wing aircraft and helicopter design. However, since the advent of evtol technology is relatively new, authentic and proper reference material for such

types of vehicles is scarce. Although there are good edifying resources for unmanned aircraft, yet there is no proper material for carrying out method-wise development for urban utility eVTOLs. Since our configuration is a combination of both fixed-wing and helicopters we cannot be dependent on one single methodology. However due to the independent propulsion systems, we can enjoy the liberty of focusing on one aspect at a time. The following section briefly describes our overall approach to the conceptual design of the vehicle.

- Most empirical formulas for fixed-wing and rotor-craft have been derived from statistical methods like curve fitting or regression. Therefore in-case of eVTOLs, it would be justified to statically choose reference values or initial values from the existing eVTOLs in the same payload or mission profile. In this regard, we have selected some of the most successful and practical Lift+Cruise designs among the directory of such types listed in [1].
- Generate a range of possible parameter values depending upon the size and energy constraints that the vehicle must follow. These ranges provide valid regions of acceptable values of parameters upon which optimization function can be defined and then finally decide upon the final values.
- In most cases the weight of the vehicle or power consumed has to be minimized. In other cases where parameter values are not directly associated with weight or energy, we design an objective function based on the design driver. This idea is properly illustrated in our airfoil selection process.
- The payload category of our air ambulance matches Kitty Hawk's Cora Design. This is an urban utility air taxi that is supposed to be commercial in near future. The vehicle has achieved many valid certifications thus making this design one of the most reliable ones in this category. Therefore we have chosen Kitty Hawk Cora as our reference aircraft. We try that our values do not deviate much from its design.
- Lastly we have followed an iterative approach in the final design selection process. Though a proper iterative code has been compiled yet, each parameter has been properly studied to ensure that results are optimal.

4 Sizing

We have followed an iterative approach in doing the sizing of the components of our vehicle. 3 shows the block diagram for the same. The baseline is MTOW(Maximum Takeoff Weight) which is initially statically determined and then finalized iteratively depending on other calculations. When all the values converge, we can then confirm the obtained values.

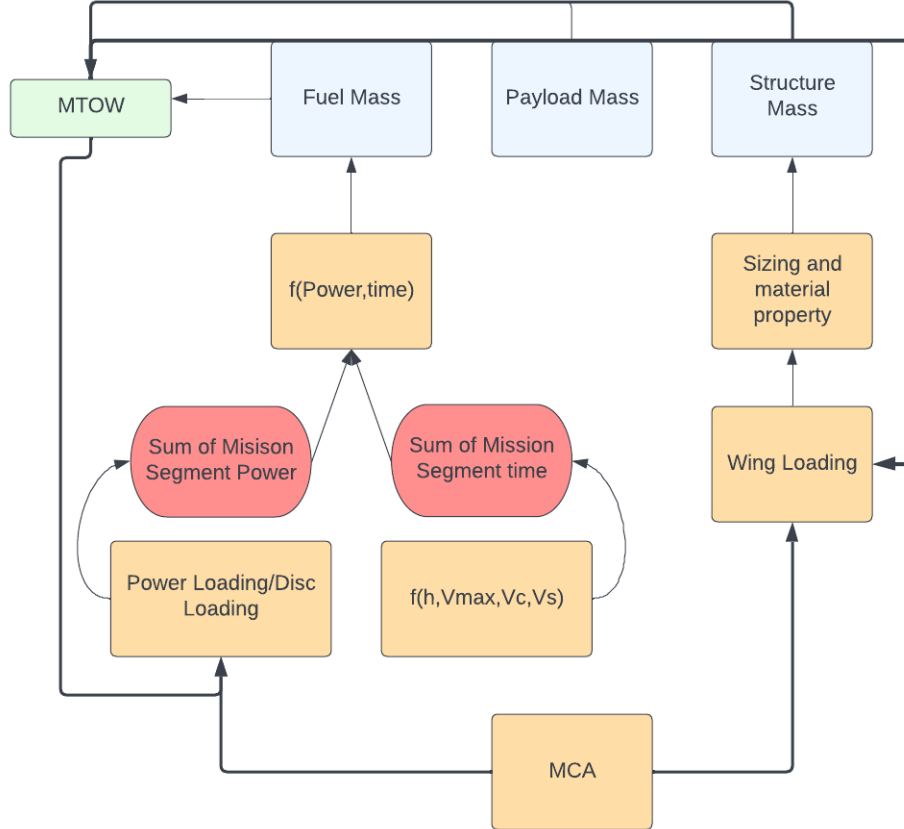


Figure 3: Iterative Sizing Procedure

5 Weight Estimation

5.1 Empirical Method

The general or traditional method for the first iteration of weight estimation is to use the weight estimate formula as done in [10]. Following are the values for various variables used in the weight estimate formula. The human payload has been taken from mission specifications, while the medical payload has been estimated from [2]. Note that values if otherwise mentioned in mission requirements are taken from historical averages of similar types of aircraft.

Weight Estimation Variables		
Designation	Variable	Values
Human Payload Weight	W_{Ph}	1666N
Medical Payload Weight	W_{Pm}	1392.6N
Total Payload Weight	W_P	3058.6N
Range	R	100km
Battery Specific Energy	e_b	250Wh/kg
Lift/Drag	L/D	7
Power Efficiency	η_P	0.8
Motor Efficiency	η_m	0.85

Table 2: Typical values for average weight fractions

The weight fraction of battery weight to take-off weight is given by:-

$$\frac{W_B}{W_{TO}} = \frac{R * g}{(L/D) * \eta_P * \eta_m * e_b * 3600} \quad (1)$$

$$\frac{W_B}{W_{TO}} = \frac{R * g}{(L/D) * \eta_P * \eta_m * e_b * 3600} = 0.23$$

The equation for estimating the empty weight is given by equation-2. We take General Aviation - twin engine(reference formula and values for A and C taken from [10])

$$A = 1.51$$

$$C = -0.10$$

$$\frac{W_E}{W_{TO}} = A W_{TO}^c K_{vs}$$

$$K_{vs} = 1.00 \quad \text{(fixed sweep)}$$

$$\frac{W_E}{W_{TO}} = (1.51)(W_{TO})^{-0.1}(1.00) = 1.51(W_{TO})^{-0.1} \quad (2)$$

The Weight Estimate equation is given by:-

$$W_{TO} = W_P + W_B + W_E \quad (3)$$

$$\begin{aligned}
W_{TO} &= W_P + W_B + W_E \\
W_{TO} &= W_P + \left(\frac{W_B}{W_{TO}}\right)W_{TO} + \left(\frac{W_E}{W_{TO}}\right)W_{TO} \\
W_P &= W_{TO} \left[1 - \left(\frac{W_B}{W_{TO}}\right) - \left(\frac{W_E}{W_{TO}}\right)\right] \\
W_{TO} &= \frac{W_P}{\left[1 - \left(\frac{W_B}{W_{TO}}\right) - \left(\frac{W_E}{W_{TO}}\right)\right]}
\end{aligned}$$

Putting in the values of ratios from above equations we get,

$$\begin{aligned}
W_{TO} &= \frac{3058.6}{\left[1 - (0.23) - (1.51W_{TO}^{-0.1})\right]} \\
W_{TO} &= \frac{3058.6}{0.77 - (1.51W_{TO}^{-0.1})}
\end{aligned}$$

We solve the above expression using iterative methods such as Newton Raphson. The converged solution gives us $W_{TO} = 15665.56N$

5.2 Statistical Method

As mentioned in the methodology section, since no theoretical formulas or expressions are available for EVTOLS, we have taken a statistical approach to estimate the maximum takeoff weight of the vehicle.

We have chosen the best current designs of the Lift+Cruise category and then averaged out the payload to the maximum take-off weight ratio. Since the only known is the total payload(human payload+medical payload) we then can obtain our MTOW.

Following is the list of Lift+Cruise evtol that we have chosen for finding out the average ratio. The reason for choosing these specific vehicles is

- Data availability for basic specifications like payload weight, Total Weight, range, etc.
- Acceptable design for valid certifications. Successful flights conducted or prototype tested. This will ensure that the data is authentic and can be brought to manufacturing.
- Developed by well-known or under the mentorship/collaboration of recognized institu-

tions. This is primarily due to the heavy importance of domain expertise in such a type of work.

The relevant data of each evtol and their ratio have been provided in the 4 given below.

Lift+Cruise Models	Payload(Kgs)	MTOW(Kgs)	Payload to MTOW ratio
VTOL Aviation India Abhiyaan ENM800	200	800	0.25
Terrafugia TF-2A (production aircraft)	200	1200	0.1666666667
SkyCAB	400	3000	0.1333333333
Aurora Flight Sciences Pegasus PAV	225	800	0.28125
Kitty Hawk Cora	181	1224	0.147875817
Average Ratio			0.1958251634

Figure 4: Payload and MTOW data for various evtols

As per the statistical method, the average comes out to be **0.1958**. This ratio can now be used to estimate the total maximum takeoff weight of the aircraft since we have already calculated the total payload expected on the vehicle. The calculations are as done below:-

$$\frac{W_P}{W_{TO}} = 0.1958$$

$$W_P = 3058.6N$$

$$W_{TO} = \frac{W_P}{0.1958} = \frac{3058.6}{0.1958}$$

$$W_{TO} = 15758.93N$$

The precise calculations(considering very high decimal precision) done using excel software are tabulated in the 5. **The final value using this method is $W_{TO} = 15780N$**

Human Payload (Kg)	170
Medical Paylaod (Kg)	142.1
Total Payload (Kg)	312.1
Design Payload to total mass ratio	0.1958251634
Design Payload Mass(kg)	312.1
Design Total Mass(kg)	1593.768618
Design MTOW(N)	15778.30932
Round Of Design MTOW(N)	15780

Figure 5: Statistical Method of estimating Weight

5.3 Conclusion

As shown in the above table, the error is a very marginal value. Therefore, we can accept our statical value and take this as our initial estimate of the total weight of the aircraft. However,

Weight Estimation Comparison	
Variable	Values
Empirical Weight Estimate	15665.56N
Statistical Weight Estimate	15780N
Error (% w.r.t empirical value)	0.72

Table 3: Table showing comparisons of weight estimate values by different methods

the reasons for considering the statistical value in contrast to empirical value due to the following reasons:-

- The Statistical Method gives more real sense to the evtol category. The theoretical formulation of weight estimate expressions for such a category can be misleading due to the high degree of diversity in possible design configurations in this category.
- The Statistical Method does not require a historical estimate of some constants, rather it is based on actually made aircraft, which gives it more belief value.
- Finally, the greater value from the statistical method gives us more margin.

6 Wing Design

In the previous section, we have estimated the most fundamental parameter of aircraft (i.e. aircraft MTOW, W_{TO}). The next step is to move in direction of wing design as this would give us an overview of the lift, drag, and sizing estimates of the aircraft.

6.1 Multi-Mode Constraints Analysis (MCA)

The first step in wing design is to get an estimate of wing planform area(S_{ref}). This is conventionally done by multi-mode constraint plots of power loading and wing loading. The performance constraints of the aircraft are expressed as a function of power-loading and wing loading. Since we are dealing with evtol, we would also have to consider the disc loading as well. For each flight phase, the constraints on performance variables such as stall speed, rate of climb, etc, can be converted into functional forms of wing loading and power loading. These equations are then plotted and the region of the curve obtained which satisfies all the equations gives us the possible values for wing loading and power loading.

The derivations of the performance equations used here can be found in [8]. In this section, we only mention the equations that we have used for our Multi-Mode constraint analysis.

Flight Modes		
Flight Mode	Constraints	Symbols
Forward Flight(FF)	Maximum Speed level flight, maximum rate of climb and stall speed	V_{max}, ROC, V_s
VTOL	Hovering, Take-off	$FOM, V_{takeoff}$

Table 4: Performance constraints for multi-mode analysis

MCA Symbols	
Symbol	Variable
PL	Power Loading
WL	Wing Loading
DL	Disc Loading
FOM	Figure of Merit
σ	solidity of VTOL propeller
C_{dblade}	Profile Drag of propeller

Table 5: Symbols used for multi-mode analysis

6.1.1 Hovering Flight

$$PL = FOM \sqrt{\frac{2\rho}{DL}} \quad (4)$$

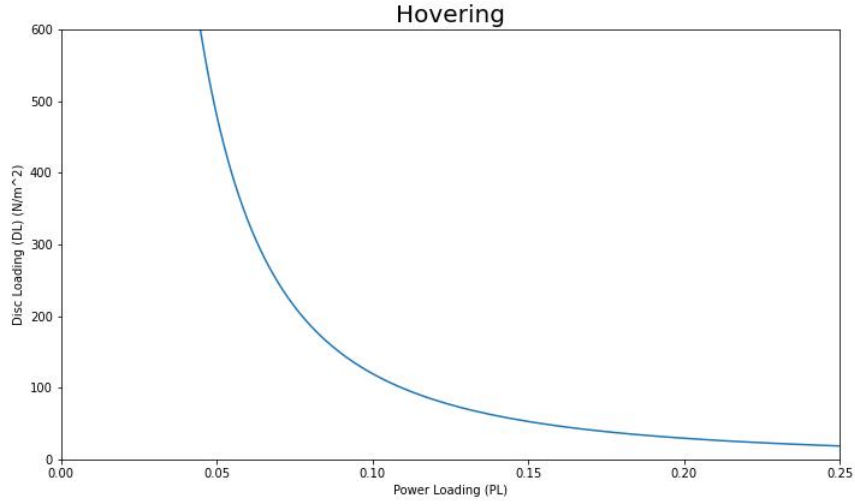


Figure 6: Performance plot for hovering phase

6.1.2 Vertical Climb Flight/Takeoff

$$PL = \frac{\sigma}{\frac{V_{takeoff}}{2} + \frac{\sqrt{V_{takeoff}^2 + \frac{2DL}{\rho_0}}}{2} + \frac{\rho_0 V_{tip}^3 \sigma C_{dblade}}{8DL} + \frac{\rho_0 V_{takeoff}^3}{DL}} \quad (5)$$

$$V_{tip} = \frac{\pi * RPM * D_{VTOL}}{60}$$

$$RPM = 2762.786 * D_{VTOL}^{-0.932}$$

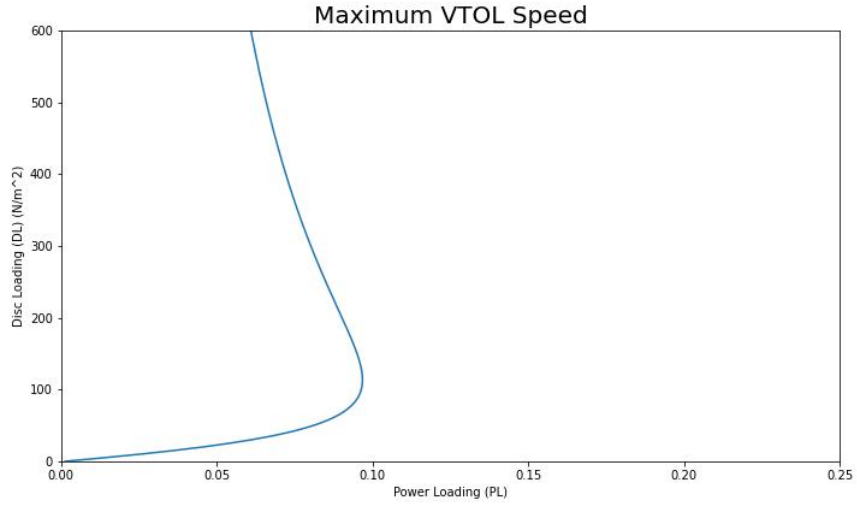


Figure 7: Performance plot for vertical climb speed

6.1.3 Stall Speed

$$WL = 0.5C_{L_{max}}\rho_0V_{stall}^2 \quad (6)$$

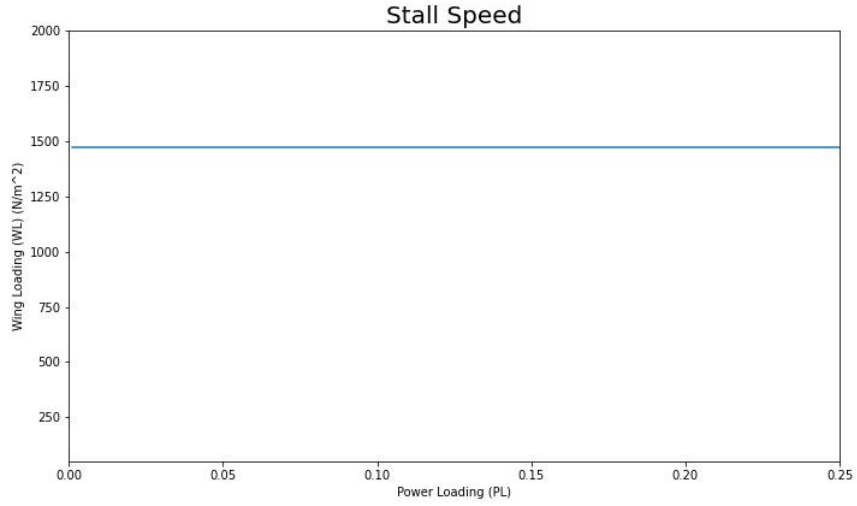


Figure 8: Performance plot for stall speed

6.1.4 Maximum Forward Speed

$$PL = \frac{\eta_{prop}}{\left[\frac{0.5\rho_0V_{max}^3C_{D0}}{WL} + \frac{2WL}{\rho_0V_{max}(\pi eAR)} \right]} \quad (7)$$

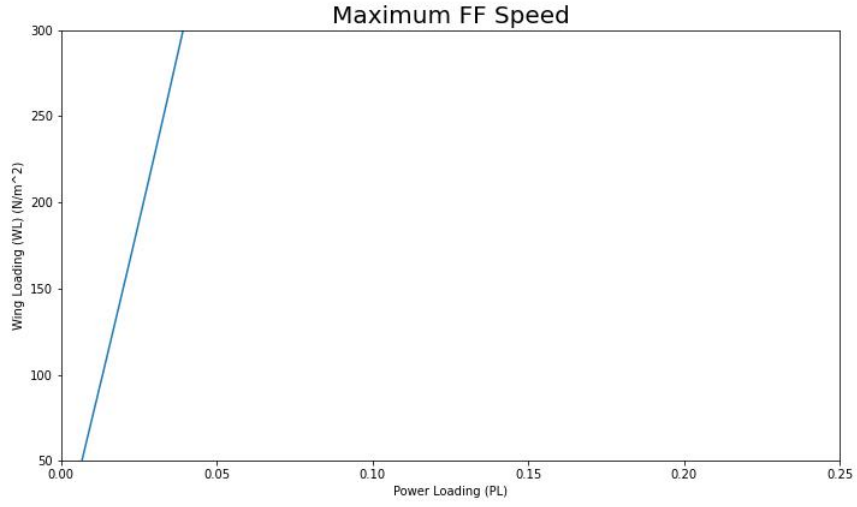


Figure 9: Performance plot for maximum forward flight speed

6.1.5 Rate of Climb

$$PL = \frac{\eta_{prop}}{\left(\frac{0.5\rho_0 V_{max}^3 C_{D0}}{WL} + \frac{2WL \cos^2(\gamma)}{\rho_0 V_c (\pi e AR)} + V_c \sin(\gamma) \right)} \quad (8)$$

$$V_c = \sqrt{\frac{2WL}{\rho_0} \sqrt{\frac{k}{3C_{D0}}}}$$

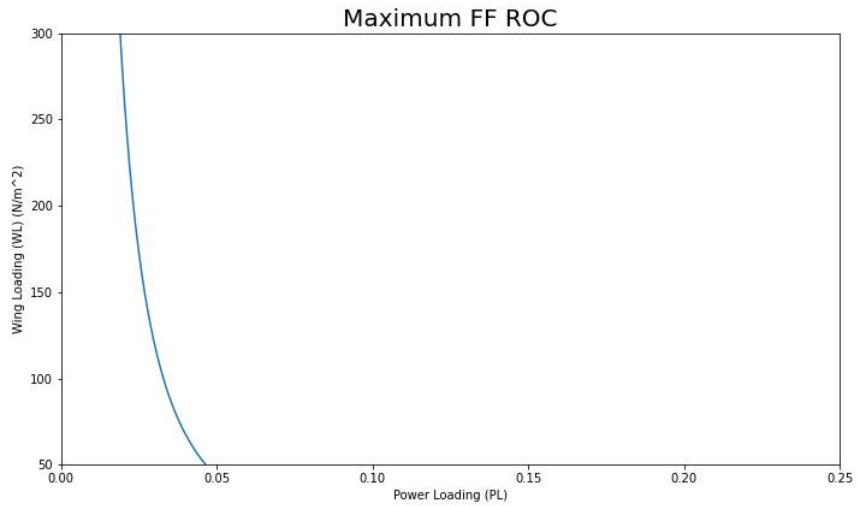


Figure 10: Performance plot for maximum rate of climb

The value for $C_{d_{blade}}$ and σ are assumed to be 0.01 and 0.077 respectively based on average data. Other values such as stall speed, the diameter of the propeller, and propeller efficiency

would also have to be assumed at this stage. Later on, we propose a new methodology that does not need assumptions on such constants and seems to be a more effective way. But it is essential to follow conventional design steps and then compare the results of any new method. Hence, we first perform MCA with the assumed values of variables given in 6.

MCA Variables	
Variable	Value
Stall Speed(V_{stall})	40m/s
Maximum Speed(V_{max})	60m/s
FOM	0.7
Diameter vertical propeller(D_{VTOL})	1.5m
σ	0.077
$C_{d_{blade}}$	0.01
C_{D_0}	0.03
Takeoff Speed($V_{takeoff}$)	0.5m/s
e	0.5
η_{prop}	0.8

Table 6: Variable values used in MCA

Combing all the performance equation plots obtained above would give us the region of selection or eligible values for power and wing loading. Since vertical flight would demand disc loading instead of wing loading, we have used two axes that simultaneously show both values for the same power loading. 11,12shows an illustration of a multi-mode constraint diagram that uses the previously specified constraint functions to graph the design space and design point. The FF mode and VTOL mode share an axis on the graph with the x-axis being PL, but the values at the design point are different. The shaded green region represents the common design space of the FF mode and the VTOL mode. All points in this region are acceptable as per theory. The designer can now choose any optimal point within this region. In general, the optimal point should be designed such that it should aim to minimize wing area and required power.

As per the classical MCA method used above, the designer can choose the initial design point. The design point would give corresponding wing loading and power loading, but since we have already done an estimate on the total weight of the aircraft, one can now get the corresponding wing reference area and power estimate(as well as disc loading).

The classical method of MCA is based on the fact that the designer has some prior on performance variable values. Usually, the detailed mission requirements or specification gives the designer these required values for MCA. However, in our scenario apart from cruise speed

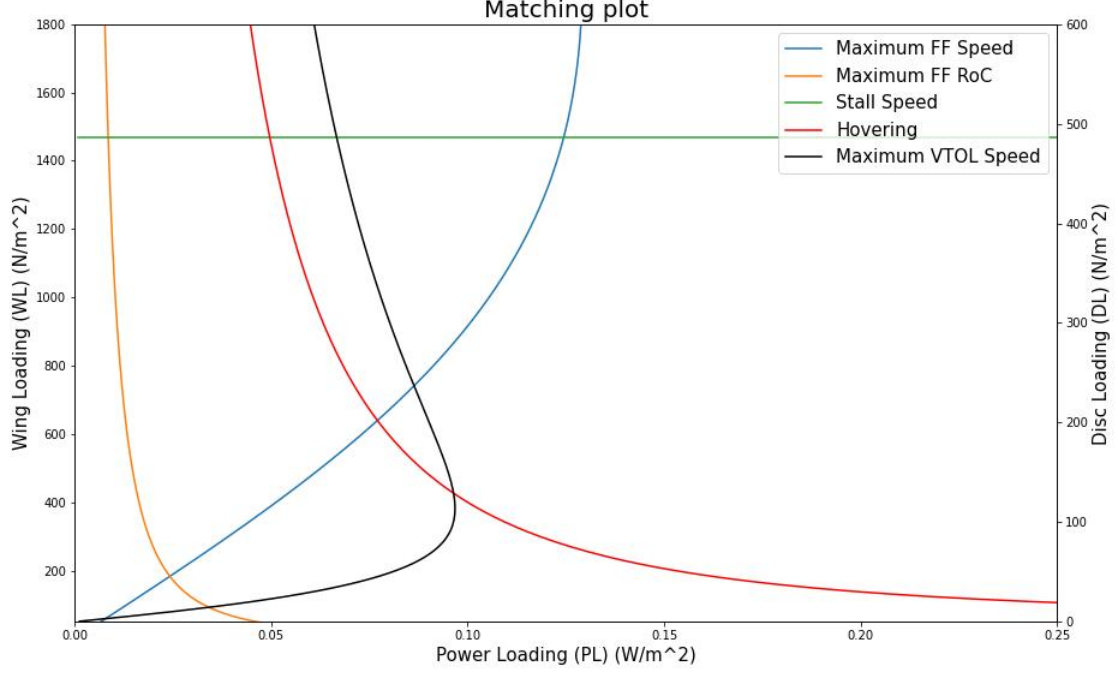


Figure 11: MCA plot

and range, none of the other values have been specified. One can only approximate them or use an average value based on historic datasets. But once again evtol is relatively a new field and very few vehicles have gone into the production or manufacturing stage. Out of those, very scarce data is available publicly. Therefore, it does not seem justifiable to rely on MCA for obtaining wing reference area.

In the next section, we propose a new method to overcome this issue. We believe that our method does not rely on too many prior assumptions and gives the designer a confidence scale to choose the optimal set of performance values.

6.2 New Proposed Method

In this section, we show a new methodology to optimally select wing reference area(S_{Ref}). The scheme is based on designing a weighted multi-variable single objective function. The procedure takes a set of weights and required performance variable values. It then gives the set of optimal values for each set of weights. The designer can then choose which set to pick based on some secondary condition such as power.

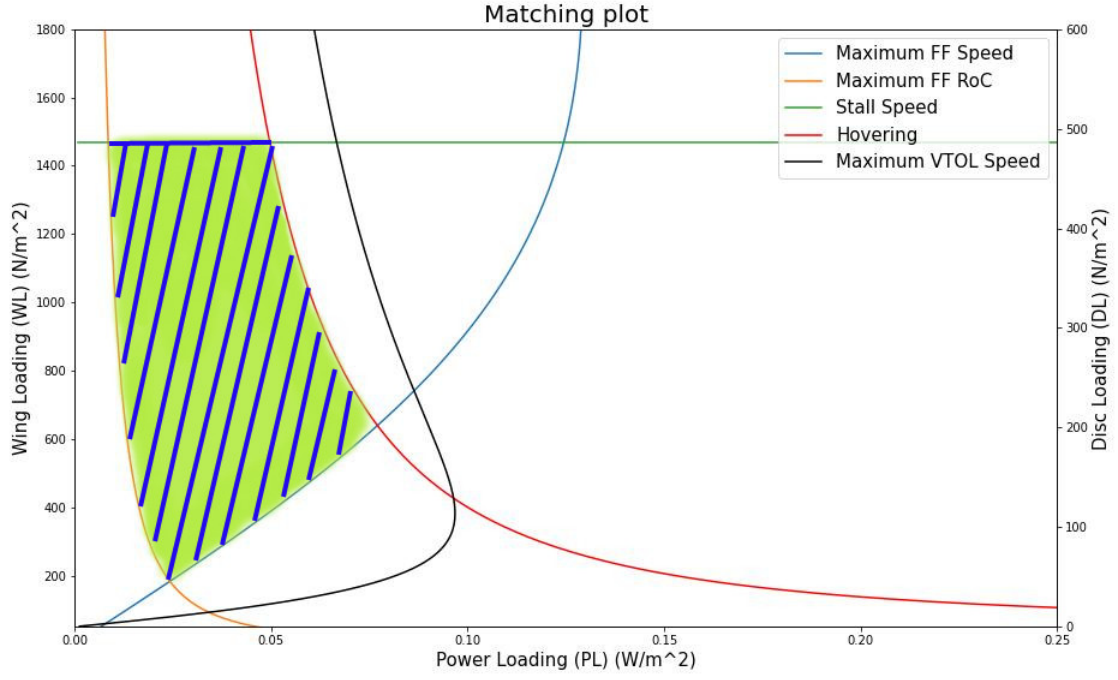


Figure 12: MCA plot with the shaded region of acceptable values.

6.2.1 Background

The method has been inspired by the airfoil selection procedure given in [10]. The procedure mentioned in the reference does calculations on lift coefficients given stall speed and cruise speed. We have been given cruise speed (V_{cruise}) as per the mission specifications, but the calculations done on the given cruise speed and estimated total weight done in the prior section, result in unreasonable values of wing area and lift coefficient. The following calculations show this trade-off:-

Given cruise speed ($V_{cruise} = V_C$) as per mission specifications:-

$$V_c = 120 km/h = 33.33 m/s$$

Estimated Total Weight (W_{TO}):-

$$W_{TO} = 15780 N$$

Aircraft Ideal Cruise Lift Coefficient (C_{L_c}) is given by:-

$$C_{L_c} = \frac{2W_{TO}}{\rho V_c^2 S}$$

The relation between aircraft ideal cruise lift coefficient and wing cruise lift coefficient ($C_{L_{cw}}$)

is dependent on the configuration of aircraft. Wing cruise lift coefficient. The lift contribution from other aircraft components like tail and fuselage will determine the actual lift shared by the wing. But since wing is the primary lift device we assume that 95% of the lift is shared by the wing alone. Therefore:-

$$C_{L_{cw}} = \frac{C_{L_c}}{0.95}$$

The wing is a 3D object. Thus there would be difference in lift generated by a 2D airfoil and that by a wing of same cross section. To account for this effect we assume that 90% of airfoil lift coefficient equals 3D lift coefficient. Thus wing airfoil ideal lift coefficient (C_{l_i}) is given by:-

$$C_{l_i} = \frac{C_{L_{cw}}}{0.9}$$

Now the actual challenge is that value of wing airfoil lift coefficient (C_{l_i}) should be in the range of (0.1 and 0.6) for all practical NACA airfoils. Reverse engineering the maximum possible value of $C_{l_i} = 0.6$ we get,

$$C_{L_{cw}} = 0.6 * 0.9 = 0.54$$

$$C_{L_c} = C_{L_{cw}} * 0.95 = 0.54 * 0.95 = 0.513$$

Using expression of aircraft ideal lift coefficient (C_{L_c}) we get,

$$C_{L_c} = \frac{2W_{TO}}{\rho V_c^2 S}$$

$$S = \frac{2W_{TO}}{\rho V_c^2 C_{L_c}}$$

As mentioned earlier, the designer must try to minimize the wing loading. Since weight is fixed this will correspond to minimizing wing area. For minimum value of wing area we should use maximum value of C_{L_c} , which we have obtained by maximum value of $C_{l_i} = 0.6$.

$$S_{min} = \frac{2W_{TO}}{\rho V_c^2 C_{L_c}} = \frac{2 * 15780}{1.225 * (33.3^2) 0.513} = 45.20m^2$$

The maximum size of overall vehicle must be within 12m as specified in sizing requirements in the problem statement. Thus we take maximum possible value of wingspan(b) = 12m. This

gives us aspect ratio(A.R.) as,

$$b_{max} = 12$$

$$AR_{max} = \frac{b_{max}^2}{S_{min}} = \frac{144}{45.20} = 3.18$$

The obtained AR is very poor for any design and the situation becomes worse as it is the maximum value for the given cruise speed. Therefore, we would have to optimally select the cruise speed as well along with stall speed. Our new proposed methodology deals with the same issue in an effective way.

6.3 Methodology

To overcome the above-illustrated challenge we came out with a method to deal with such an issue. We design a weighted multi-variable objective function. The function results in a set of optimal values. Depending on the constraints and reasonable values of performance variables we then filter out the eligible set of values for our purpose. Finally, we pass on these values to another objective function which gives us the final set of values. 13 is a block diagram illustrating the scheme.

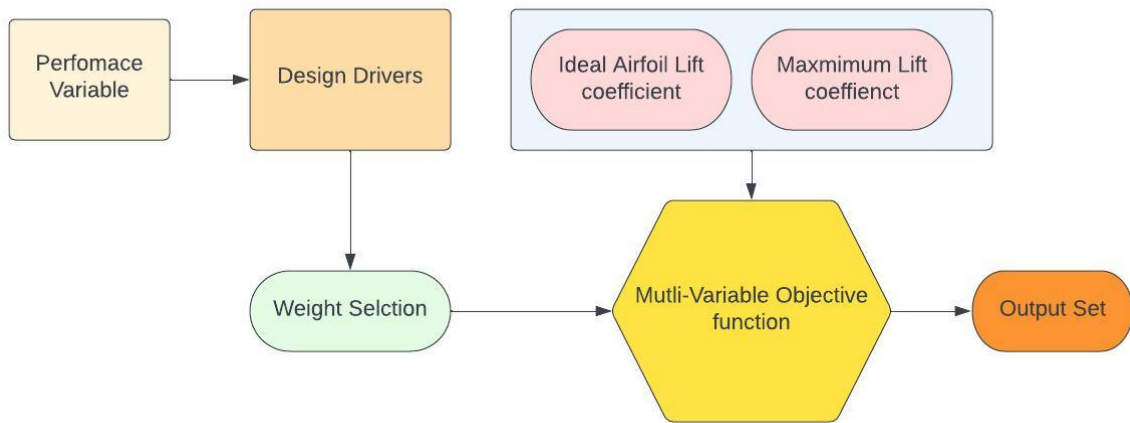


Figure 13: Block Diagram showing Performance variable selection for obtaining wing area

As shown in the above expressions for lift coefficients, we need to get the value of density at our design cruise altitude. The calculations primarily need density value at sea level and cruise altitude. Density is a function of altitude and therefore we need to decide the cruise altitude.

International Civil Aviation Organization[3] specifies the safety margin for any aerial vehicle to be at least 304.8m above the tallest building in the area of flight. The tallest building in

India is Palais Royale which has a height of about 320m. Therefore safety altitude should be $320 + 304.8 = 624.8m$. The figure14 shows the relevant numbers for the same.

Tallest building height in India(m)	320
International Civil Aviation Organization safety margin(m)	304.8
Safety Altitude (m)	624.8
Design Altitude(m)	650
Density at design altitude(SI units)	1.185

Figure 14: Cruise altitude and density

Thus our **density at cruise altitude** (ρ_c) = $1.185kg/m^3$.

We have three variables that have trade-offs among them for lift coefficient values. That are stall speed, cruise speed, and wing area ($[V_c, V_s, S]$). While stall speed and wing area should be minimized cruise speed should be maximized. Therefore we need to assign a priority index to these three variables to set our objective function. These priority indexes or weights can either be designer specific or derived from mission requirements. However, we believe that we can incorporate our detailed study about design drivers for choosing weights.

Usually one of the performance variables directly impacts one or more than one design driver. For example, speed is a function of cruise speed. The more the cruise speed, the faster the system. Similarly, size can be matched to wing area and safety can be linked to the safety of the vehicle.

Design Drivers	Parameter Associated	Weight
Safety	Stall Speed	0.5
Speed	Cruise Speed	0.3333333333
Size	Wingspan area	0.1666666667

Figure 15: Design Drivers and their related variables

Depending upon the relative priority of design drivers, the weights were roughly calculated as the ones given in the 15. However to ensure the best set of possible values we also decided to vary the weights, i.e. we obtained a different set of optimal values for a different set of weights.

5 sets of weights have been used. They are listed in the table[10].

The airfoil ideal lift coefficient C_{l_i} varies between $[0.1, 0.6]$. The value of C_{l_i} is a function of cruise speed and wing area as density and weight have already been fixed. Therefore we can obtain a curve for cruise speed v/s wing area for a different sets of ideal airfoil lift coefficients and analyze the trade-off. The fig16 shows this variation.

Weights		
Weight Set no.	Variables	Weights
1	$[V_{stall}, V_{Cruise}, S_{ref}]$	$[2.0, -1.5, 1.0]$
2	$[V_{stall}, V_{Cruise}, S_{ref}]$	$[2.5, -1.5, 1.0]$
3	$[V_{stall}, V_{Cruise}, S_{ref}]$	$[3.0, -1.5, 1.0]$
4	$[V_{stall}, V_{Cruise}, S_{ref}]$	$[3.5, -1.5, 1.0]$
5	$[V_{stall}, V_{Cruise}, S_{ref}]$	$[4.0, -1.5, 1.0]$

Table 7: Different set of weights configuration used. Note that cruise speed has negative weight as it has to be minimized

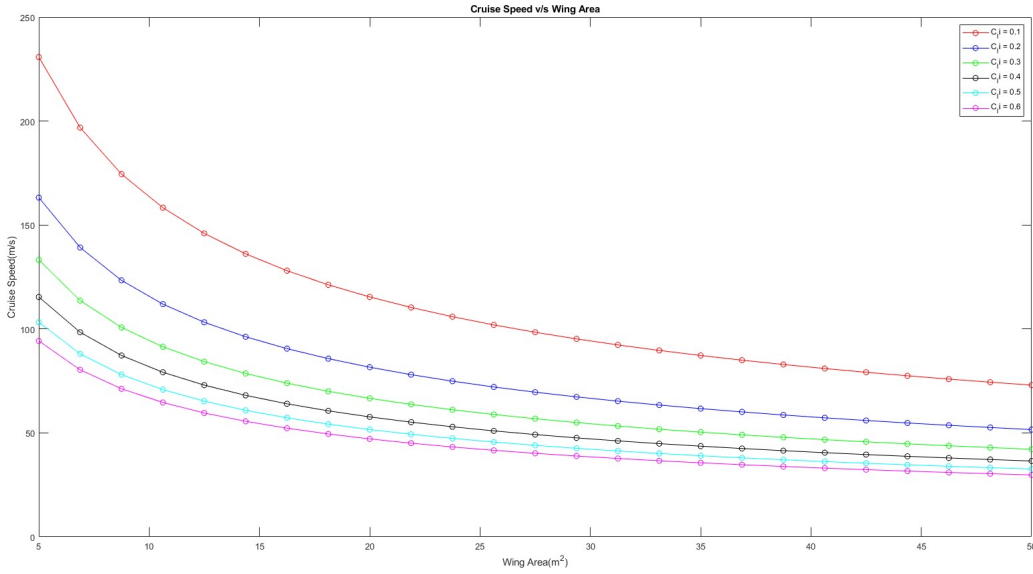


Figure 16: Variation of cruise speed v/s wing area for a given C_{li}

As can be seen from the plot, the relationship is inverse. The lesser the wing area the more the cruise speed for a given C_{li} . Also increasing the value of C_{li} gives more cruise speed for a given wing area. Thus it becomes obvious to select the least possible wing area and therefore highest cruise speed. But since wing area has a relation with stall speed as well for maximum lift coefficient, we need to analyze their trade-off as well. The fig17 shows this variation.

The relation between stall speed and the wing area is the same as that of cruise speed v/s wing area. However, where we desire greater cruise speed, we require less stall speed for safety purposes. Less stall speed will require less speed for the maximum lift required to safely glide the plane. The air ambulance design needs to be very safe due to the critical condition of the patient inside. Thus stall speed needs to have more weightage as compared to cruise speed and wing area. This can be seen from our weight sets shown in table[9].

Thus now we have a clear understanding of the dilemma we are facing. We want high cruise speed and therefore can get less wing area, but simultaneously for the given wing area we

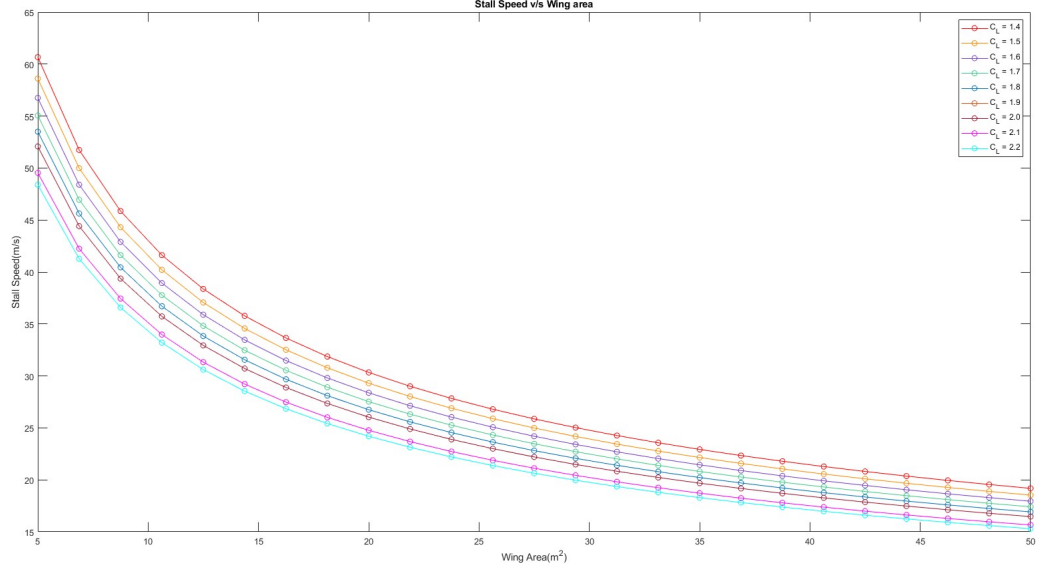


Figure 17: Variation of stall speed v/s wing area for a given C_L

would get high stall speed. Therefore we need to set an objective function with weights assigned to all the variables (V_s, V_c, S). The objective function would give us optimal values of these variables for a given C_{li} and C_L .

Our objective function is a simple weighted average of the stall speed, cruise speed, and wing area. The function is as follows:-

$$f = \arg \min_{(V_s, V_c, S)} \frac{w_1 V_s + w_2 V_c + w_3 S}{w_1 + |w_2| + w_3} \quad (9)$$

The absolute value of w_2 is taken because the weight is negative in value as we need the maximum value of cruise speed possible. The range of different variables(wing area and lift coefficients) taken are shown in table8.

Range of Values		
Variable	Symbol	Range
Wing Area(m^2)	S_{ref}	[5,33]
Wing airfoil ideal lift coefficient	C_{li}	[0.1,0.6]
Aircraft maximum lift coefficient	C_L	[1.8, 2.2]

Table 8: Range of values for lift coefficients and wing area

The obtained value sets for each configuration of weights and C_{li} , C_L values are shown in the figures1819202122.

The tables show an optimal set of values for the mentioned configuration, We have highlighted the chosen sets based on some underlying constraints. We have neglected those val-

Design C_L	1.8				
Design C_li	Weights-1	Weight-2	Weights-3	Weights-4	Weights-5
	[2.0, -1.5, 1.0]	[2.5, -1.5, 1.0]	[3.0, -1.5, 1.0]	[3.5, -1.5, 1.0]	[4.0, -1.5, 1.0]
0.1	[53.50, 230.79, 5.0]	[53.50, 230.79, 5.0]	[53.50, 230.79, 5.0]	[53.50, 230.79, 5.0]	[53.50, 230.79, 5.0]
0.2	[53.50, 163.19, 5]	[53.50, 163.19, 5]	[53.50, 163.19, 5]	[53.50, 163.19, 5]	[53.50, 163.19, 5]
0.3	[53.50, 133.24, 5]	[53.50, 133.24, 5]	[53.50, 133.24, 5]	[53.50, 133.24, 5]	[46.33, 115.39, 6.66]
0.4	[53.50, 115.39, 5]	[53.50, 115.39, 5]	[53.50, 115.39, 5]	[46.33, 99.93, 6.66]	[34.01, 73.37, 12.36]
0.5	[53.5, 103.21, 5]	[53.5, 103.21, 5]	[53.5, 103.21, 5]	[36.24, 69.92, 10.89]	[29.19, 56.32, 16.78]
0.6	[53.5, 94.22, 5.0]	[53.5, 94.22, 5.0]	[42.43, 74.73, 7.94]	[32.15, 56.62, 13.84]	[27.99, 49.29, 18.26]

Figure 18: Optimal set of values for $C_L = 1.8$

Design C_L	1.9				
Design C_li	Weights-1	Weight-2	Weights-3	Weights-4	Weights-5
	[2.0, -1.5, 1.0]	[2.5, -1.5, 1.0]	[3.0, -1.5, 1.0]	[3.5, -1.5, 1.0]	[4.0, -1.5, 1.0]
0.1	[53.50, 230.79, 5.0]	[53.50, 230.79, 5.0]	[53.50, 230.79, 5.0]	[53.50, 230.79, 5.0]	[53.50, 230.79, 5.0]
0.2	[53.50, 163.19, 5]	[53.50, 163.19, 5]	[53.50, 163.19, 5]	[53.50, 163.19, 5]	[53.50, 163.19, 5]
0.3	[53.50, 133.24, 5]	[53.50, 133.24, 5]	[53.50, 133.24, 5]	[53.50, 133.24, 5]	[46.33, 115.39, 6.66]
0.4	[53.50, 115.39, 5]	[53.50, 115.39, 5]	[53.50, 115.39, 5]	[46.33, 99.93, 6.66]	[35.27, 78.17, 10.89]
0.5	[53.5, 103.21, 5]	[53.5, 103.21, 5]	[53.5, 103.21, 5]	[37.93, 75.19, 9.42]	[29.75, 58.97, 15.31]
0.6	[53.5, 94.22, 5.0]	[53.5, 94.22, 5.0]	[45.76, 82.80, 6.47]	[33.11, 59.09, 12.36]	[27.24, 49.29, 18.26]

Figure 19: Optimal set of values for $C_L = 1.9$

ues which have cruise speed greater than 80m/s and wing area more than $15m^2$. This is due to the practicality of design. A very high cruise speed would require a very high amount of energy, moreover, the specified cruise speed is about 33.33m/s. So we should not go in regions of high cruise speed. Thus we have filtered out the optimal set(green points).

The next step is to send these values into a second objective function and then finally obtain the one optimal set. In our case, we have chosen the total power estimate in forward flight (level flight+climb flight) as our primary condition to get the optimal value. We have estimated the total power using the MCA equations mentioned in previous sections. The Ostwald's factor of efficiency(e) has been calculated using

$$e = 1.78(1 - 0.045AR^{0.68}) - 0.64 \quad (10)$$

Rest calculations have been done as shown in the MCA section. The plot of the total power estimate in forward flight is shown in fig23.

One more constraint that should be considered is the aspect ratio(AR). The aerodynamics of the wing would not be efficient if the value of AR is very less. From the average values of AR found in manufactured or prototype evtols, we have used the baseline AR to be 7, i-e we

Design C_L	2				
Design C_li	Weights-1	Weight-2	Weights-3	Weights-4	Weights-5
	[2.0, -1.5, 1.0]	[2.5, -1.5, 1.0]	[3.0, -1.5, 1.0]	[3.5, -1.5, 1.0]	[4.0, -1.5, 1.0]
0.1	[53.50, 230.79, 5.0]	[53.50, 230.79, 5.0]	[53.50, 230.79, 5.0]	[53.50, 230.79, 5.0]	[53.50, 230.79, 5.0]
0.2	[53.50, 163.19, 5]	[53.50, 163.19, 5]	[53.50, 163.19, 5]	[53.50, 163.19, 5]	[53.50, 163.19, 5]
0.3	[53.50, 133.24, 5]	[53.50, 133.24, 5]	[53.50, 133.24, 5]	[53.50, 133.24, 5]	[46.33, 115.39, 6.66]
0.4	[53.50, 115.39, 5]	[53.50, 115.39, 5]	[53.50, 115.39, 5]	[46.33, 99.93, 6.66]	[34.38, 78.17, 10.89]
0.5	[53.5, 103.21, 5]	[53.5, 103.21, 5]	[53.5, 103.21, 5]	[36.97, 75.19, 9.42]	[30.50, 62.03, 13.84]
0.6	[53.5, 94.22, 5.0]	[53.5, 94.22, 5.0]	[50.75, 94.22, 5]	[32.27, 59.90, 12.36]	[27.69, 51.41, 16.78]

Figure 20: Optimal set of values for $C_L = 2.0$

Design C _L	2.1				
Design C _{li}	Weights-1	Weight-2	Weights-3	Weights-4	Weights-5
	[2.0, -1.5, 1.0]	[2.5, -1.5, 1.0]	[3.0, -1.5, 1.0]	[3.5, -1.5, 1.0]	[4.0, -1.5, 1.0]
0.1	[53.50, 230.79, 5.0]	[53.50, 230.79, 5.0]	[53.50, 230.79, 5.0]	[53.50, 230.79, 5.0]	[53.50, 230.79, 5.0]
0.2	[53.50, 163.19, 5]	[53.50, 163.19, 5]	[53.50, 163.19, 5]	[53.50, 163.19, 5]	[53.50, 163.19, 5]
0.3	[53.50, 133.24, 5]	[53.50, 133.24, 5]	[53.50, 133.24, 5]	[53.50, 133.24, 5]	[46.33, 115.39, 6.66]
0.4	[53.50, 115.39, 5]	[53.50, 115.39, 5]	[53.50, 115.39, 5]	[46.33, 99.93, 6.66]	[36.08, 84.06, 9.42]
0.5	[53.5, 103.21, 5]	[53.5, 103.21, 5]	[53.5, 103.21, 5]	[39.28, 81.86, 7.94]	[29.77, 62.03, 13.84]
0.6	[53.5, 94.22, 5.0]	[53.5, 94.22, 5.0]	[50.75, 94.22, 5]	[33.55, 63.83, 10.89]	[28.30, 53.83, 15.31]

Figure 21: Optimal set of values for $C_L = 2.1$

Design C _L	2.2				
Design C _{li}	Weights-1	Weight-2	Weights-3	Weights-4	Weights-5
	[2.0, -1.5, 1.0]	[2.5, -1.5, 1.0]	[3.0, -1.5, 1.0]	[3.5, -1.5, 1.0]	[4.0, -1.5, 1.0]
0.1	[53.50, 230.79, 5.0]	[53.50, 230.79, 5.0]	[53.50, 230.79, 5.0]	[53.50, 230.79, 5.0]	[53.50, 230.79, 5.0]
0.2	[53.50, 163.19, 5]	[53.50, 163.19, 5]	[53.50, 163.19, 5]	[53.50, 163.19, 5]	[53.50, 163.19, 5]
0.3	[53.50, 133.24, 5]	[53.50, 133.24, 5]	[53.50, 133.24, 5]	[53.50, 133.24, 5]	[46.33, 115.39, 6.66]
0.4	[53.50, 115.39, 5]	[53.50, 115.39, 5]	[53.50, 115.39, 5]	[46.33, 99.93, 6.66]	[38.83, 91.53, 7.94]
0.5	[53.5, 103.21, 5]	[53.5, 103.21, 5]	[53.5, 103.21, 5]	[42.53, 90.70, 6.47]	[30.77, 65.62, 12.36]
0.6	[53.5, 94.22, 5.0]	[53.5, 94.22, 5.0]	[50.75, 94.22, 5]	[35.25, 68.64, 9.42]	[27.65, 53.83, 15.31]

Figure 22: Optimal set of values for $C_L = 2.2$

TOTAL Power(KW) vs. Point No.

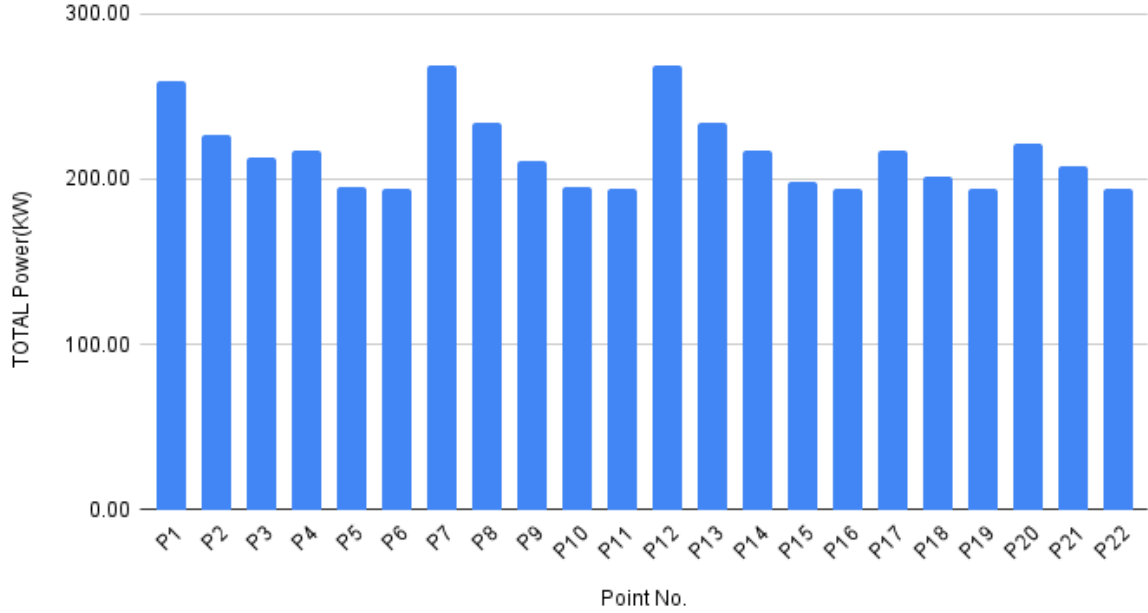


Figure 23: Power v/s Optimal set of points. Note that range of estimated total power is very close to the forward flight power mentioned for Kitty Hawk Cora in ref[2]

reject those points which have AR less than 7. The blue highlighted points are the points that have power less than the red point, but since the red point(P10) has the minimum power that has AR greater than 7. We have finally selected the point(P10) as our final optimal point.

We now have obtained wing area, aspect ratio, and estimates on ideal and maximum lift coefficients. The designer is ensured about the optimality of these results as we have shown the detailed trade-off analysis at each step. We now head to the airfoil selection process.

Final Values	
Variable	Value
Airfoil Ideal lift coefficient(C_{li})	0.6
Aircraft maximum lift coefficient(C_L)	1.9
Wing Area(S_{ref})	$12.8m^2$
Wingspan(b)	10m
Aspect ratio(AR)	7.81
Chord length(MAC)	1.28m
Cruise Speed	58.8m/s
Stall Speed	32.5m/s

Table 9: Values of variables obtained by the proposed method

Point No	C _L	C _D	V _{stall}	V _{cruise}	S _{ref}	V _{max}	WL	AR	C _D not	rho	e	neta _{prop}	climb angle	V _c	PL _{ff} level	P _{ff} level(W)	PL _{ff} climb	P _{ff} climb(W)	TOTAL Power(KW)
P1	1.8	0.4	34.01	73.37	12.26	80.707	1287.11	8.16	0.03	1.225	0.81	0.8	0.02136	30.90	0.0913	172906.69	0.1829	86259.67	259.17
P2	1.8	0.5	36.24	69.92	10.89	76.912	1449.04	9.18	0.03	1.225	0.78	0.8	0.02136	33.48	0.1120	140840.72	0.1844	85581.87	226.42
P3	1.8	0.5	29.19	56.32	16.78	61.952	940.41	5.96	0.03	1.225	0.87	0.8	0.02136	24.89	0.1297	121656.64	0.1732	91097.68	212.75
P4	1.8	0.6	42.43	74.73	7.94	82.203	1987.41	12.59	0.03	1.225	0.69	0.8	0.02136	41.19	0.1216	129773.70	0.1816	86891.65	216.67
P5	1.8	0.6	32.15	56.82	13.84	62.282	1140.17	7.23	0.03	1.225	0.83	0.8	0.02136	28.44	0.1461	100808.49	0.1901	87602.66	195.61
P6	1.9	0.6	27.96	49.29	18.26	54.219	864.18	5.48	0.03	1.225	0.89	0.8	0.02136	23.46	0.1569	100560.60	0.1694	93167.82	193.73
P7	1.9	0.4	35.27	78.17	10.89	85.987	1449.04	9.18	0.03	1.225	0.78	0.8	0.02136	33.48	0.0961	183209.97	0.1844	85581.87	268.79
P8	1.9	0.5	37.93	75.19	9.42	82.709	1675.16	10.62	0.03	1.225	0.74	0.8	0.02136	36.86	0.1060	148835.25	0.1843	85612.15	234.45
P9	1.9	0.5	29.75	58.17	15.31	63.987	1030.70	6.53	0.03	1.225	0.85	0.8	0.02136	26.53	0.1296	121777.99	0.1769	89224.26	211.00
P10	1.9	0.6	33.15	59.26	12.36	64.566	1238.16	8.08	0.03	1.225	0.81	0.8	0.02136	30.73	0.1451	108774.56	0.1838	86325.13	195.10
P11	1.9	0.6	27.24	49.29	18.26	54.219	864.18	5.48	0.03	1.225	0.89	0.8	0.02136	23.46	0.1569	100560.60	0.1694	93167.82	193.73
P12	2	0.4	34.38	78.17	10.89	85.987	1449.04	9.18	0.03	1.225	0.78	0.8	0.02136	33.48	0.0961	183209.97	0.1844	85581.87	268.79
P13	2	0.5	36.97	75.19	9.42	82.709	1675.16	10.62	0.03	1.225	0.74	0.8	0.02136	36.86	0.1060	148835.25	0.1843	85612.15	234.45
P14	2	0.5	30.5	62.03	13.84	68.233	1140.17	7.23	0.03	1.225	0.83	0.8	0.02136	28.44	0.1219	129471.63	0.1901	87602.66	217.07
P15	2	0.6	32.27	59.9	12.36	65.89	1276.70	8.09	0.03	1.225	0.81	0.8	0.02136	30.73	0.1414	111607.53	0.1828	86329.13	197.94
P16	2	0.6	27.69	51.41	16.78	56.651	940.41	5.96	0.03	1.225	0.87	0.8	0.02136	24.89	0.1538	102583.86	0.1732	91097.68	193.68
P17	2.1	0.5	29.77	62.03	13.84	68.233	1140.17	7.23	0.03	1.225	0.83	0.8	0.02136	28.44	0.1219	129471.63	0.1901	87602.66	217.07
P18	2.1	0.6	33.55	63.83	10.89	70.213	1449.04	9.18	0.03	1.225	0.78	0.8	0.02136	33.48	0.1358	116199.20	0.1844	85581.87	201.78
P19	2.1	0.6	28.3	53.83	15.31	59.213	1030.70	6.53	0.03	1.225	0.85	0.8	0.02136	26.53	0.1502	105048.25	0.1769	89224.26	194.27
P20	2.2	0.5	30.77	65.62	12.36	72.162	1276.70	8.09	0.03	1.225	0.81	0.8	0.02136	30.73	0.1173	134515.35	0.1828	86329.13	220.84
P21	2.2	0.6	35.25	68.64	9.42	75.504	1675.16	10.62	0.03	1.225	0.74	0.8	0.02136	36.86	0.1293	122059.56	0.1843	85612.15	207.68
P22	2.2	0.6	27.65	53.83	15.31	59.213	1030.70	6.53	0.03	1.225	0.85	0.8	0.02136	26.53	0.1502	105048.25	0.1769	89224.26	194.27

Figure 24: Final Optimal set of values

6.4 Airfoil Selection

We follow the classical airfoil selection as done in [10]. We already have our wing airfoil ideal lift coefficient (C_{li}) and aircraft maximum lift coefficient (C_L or $C_{L_{max}}$). We just need to obtain the airfoil maximum lift coefficient ($C_{l_{max}}$). For this, we need to get an estimate of the lift coefficient of high lift device, but at this stage we assume this value to be 0.8 ($\Delta C_{HLD} = 0.8$) Calculations for airfoil maximum lift coefficient: Given Aircraft Maximum Lift Coefficient:-

$$C_{L_{max}} = 1.9$$

Wing maximum lift coefficient:-

$$C_{L_{maxw}} = \frac{C_{L_{max}}}{0.95} = 2.0$$

Wing airfoil gross maximum lift coefficient:-

$$C_{l_{maxgross}} = \frac{C_{L_{maxw}}}{0.9} = 2.22$$

Wing airfoil net maximum lift coefficient:-

$$C_{l_{max}} = C_{l_{max_{gross}}} - \Delta C_{HLD} = 2.22 - 0.8 = 1.42$$

Therefore, we now need to look for NACA airfoil sections that can yield an ideal lift coefficient of 0.6 and a net maximum lift coefficient of 1.42.

From the database of NACA-6 digit airfoils, we find only two NACA airfoil that satisfies our requirements($C_{l_i} = 0.6$ and $C_{l_{max}}$ greater than 1.42). They are NACA 63(3)-618 and NACA63(2)-615. The four major aerodynamic plots for both these airfoils have been obtained using xflr5. They have been obtained on $Re = 5.7e+06$ and $mach=0.19$. Both of these have been calculated based on cruise speed and wing chord length.

Figure30 shows a comparison in terms of numeric values derived from the aerodynamic plots of this airfoil. From the data, we can conclude that the most appropriate airfoil for our purpose would be NACA 63(3)-618 because of its good stall quality over NACA 63(2)-615.

Since our design driver safety had the most priority, major importance would go to stall characteristics and hence the choice. **Thus our airfoil for wing is NACA 63(3)-618.**

	Stall Angle(alpha_s)	Maximum Lift Coefficient	Zero Lift angle	Ideal Lift Coeff	zero lift coeff	lift/alpha slope	Stall characteristic	C_m	C_dmin	(Cl/Cd)max
NACA 63(3)-618	22.17	1.46	-4.44	0.6	0.546	0.122972973	Good [-0.121, -0.025]		0.005	101.93
NACA 63(2)-615	19.45	1.59	-4.44	0.6	0.538	0.1211711712	Okay [-0.121, -0.029]		0.005	108.278

Figure 25: Comparison among possible airfoil candidates

6.5 3D Wing Design

For analysis the aerodynamic properties for the wing, XFLR5 software is used. The method employed is Lifting Line Theory(LLT). The hypothesis upon which the theory is based is that a lifting wing can be replaced by a lifting line and that the incremental vortices shed along the span trail behind the wing in straight lines in the direction of the freestream velocity.

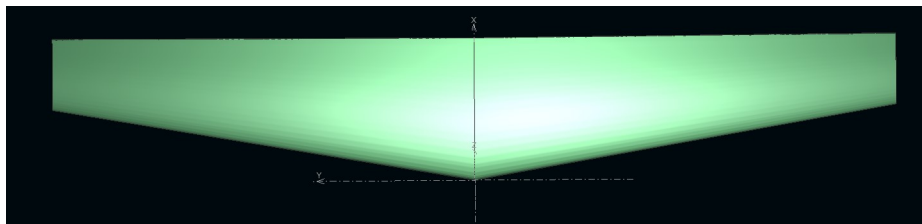


Figure 26: 3D wing modeled in XFLR5

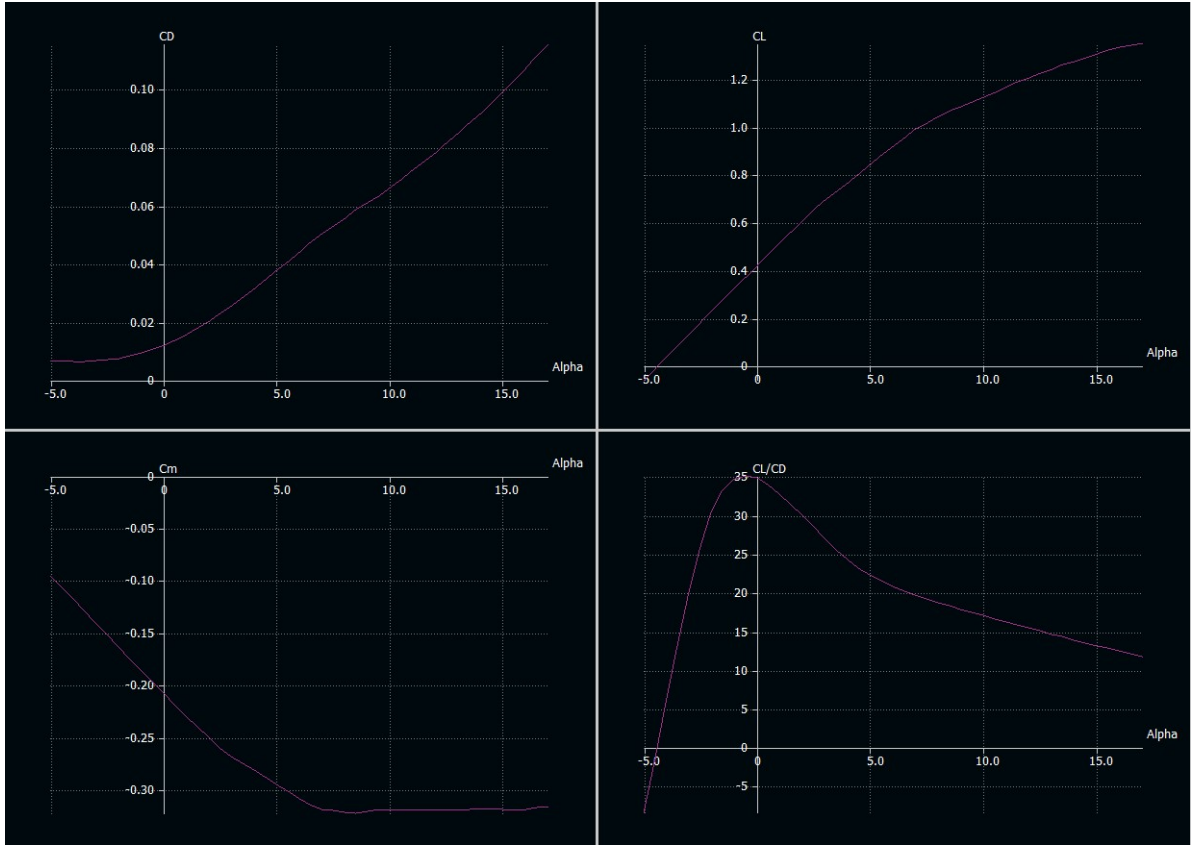


Figure 27: Coefficients for 3D Wing using LLT in XFLR5

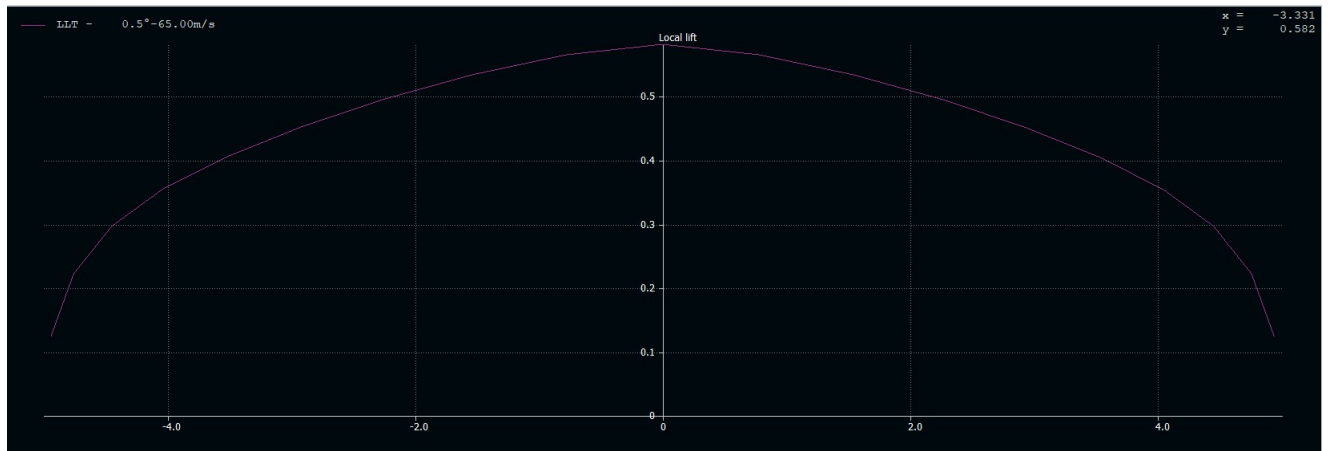


Figure 28: Lift Distribution over the wing

7 Tail Design

We have taken a conventional aft horizontal tail and one aft vertical tail for our design. The primary reason for this choice is due to its simplicity, ease of design, and safety. We have followed the design steps and done in [10]. For two-seater GA aircraft, the tail volume coefficient is assumed to be 0.65.

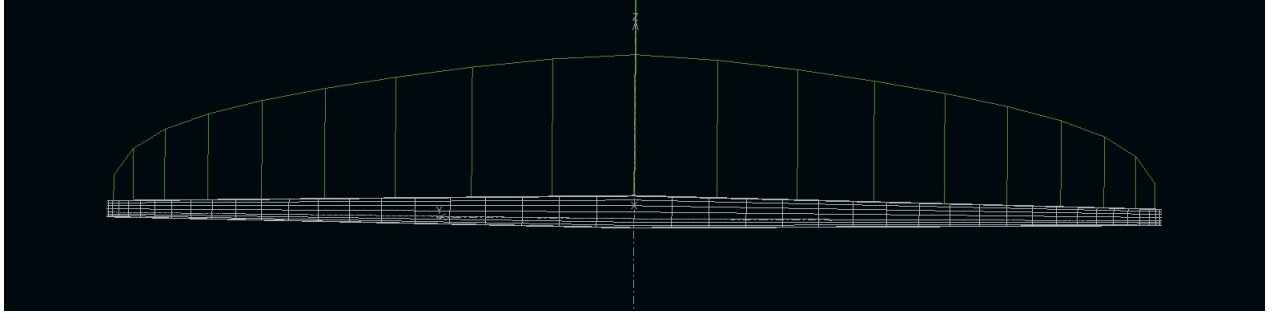


Figure 29: Elliptical Distribution of Lift

$$\bar{V}_H = 0.65 \quad (11)$$

The maximum fuselage diameter has been taken to be 2.4m based on the max cabin dimensions specified.

$$\begin{aligned} l_{opt} &= K_c \frac{\sqrt{4\bar{C}S\bar{V}_H}}{\sqrt{\pi D_f}} \\ &= 1.4 \frac{\sqrt{4 * 1.28 * 12.8 * 0.65}}{\pi 2.4} = 3.32m \end{aligned}$$

The tail planform area is determined as:

$$\begin{aligned} \bar{V}_H &= \frac{l\bar{S}_h}{\bar{C}S} \\ \bar{S}_h &= \frac{\bar{C}S\bar{V}_H}{l} \\ &= \frac{1.28 * 12.8 * 0.65}{3.32} = 3.2m^2 \end{aligned}$$

Our aircraft cruise lift coefficient is:

$$C_{Lc} = 0.6$$

The wing/fuselage aerodynamic pitching moment coefficient is:

$$\begin{aligned} C_{m_{owf}} &= C_{m_{af}} \frac{AR \cos^2(\Lambda)}{AR + 2 \cos(\Lambda)} + 0.01\alpha_t \\ &= -0.12 \frac{7.8 \cos^2(9.70)}{7.8 + 2 \cos(9.70)} + 0.01(0) = -0.09 \end{aligned}$$

TRIM EQUATIONS

$$\begin{aligned} L_f &= \frac{l_{opt}}{0.65} \\ &= 3.32/0.65 = 5.10 \end{aligned}$$

The aerodynamic center of the wing/fuselage combination is located at 0.23 of MAC, and the aircraft center of gravity is located at 0.3 of the fuselage length. This cg is 7 cm ahead of the wing/fuselage aerodynamic center.

$$\begin{aligned} X_{apex} + 0.23MAC &= 0.3L_f + 0.07 \\ &= 1.29m \end{aligned}$$

C.G. calculation

$$\begin{aligned} X_{cg} &= 0.23MAC - 0.07 = 0.23(1.33) - 0.07 = 0.23m \\ \bar{X}_{cg} = h &= \frac{0.23}{1.33} = 17\%MAC \end{aligned}$$

Assuming tail lift efficiency to be 0.98.

$$\begin{aligned} C_{m_{owf}} + C_L(h - h_o) - \eta_h \bar{V}_H C_{L_h} &= 0 \\ C_{L_h} &= \frac{C_{m_{owf}} + C_L(h - h_o)}{\eta_h \bar{V}_H} \\ &= \frac{-0.09 + 0.6(0.17 - 0.23)}{0.65 * 0.98} \\ C_{L_h} &= -0.19 \end{aligned}$$

We have chosen NACA-0009 as the airfoil for our tail. The value of various parameters related to it are given in fig

C_{l_i}	$C_{d_{min}}$	C_m	$(C_l/C_d)_{max}$	α_o (deg)	α_s (deg)	$C_{l_{max}}$	C_{l_α} (1/rad)	$(t/c)_{max}$
0	0.005	0	83.3	0	13	1.3	6.7	9%

Figure 30: NACA 0009 airfoil data. Taken from [10]

$$C_{L_{\alpha h}} = \frac{6.7}{1 + \frac{6.7}{\pi 5.2}} = 4.761/rad$$

The tail angle of attack in cruise is:

$$\begin{aligned}\alpha_h &= \frac{C_{L_h}}{C_{L_{\alpha h}}} \\ &= \frac{-0.19}{4.76} = -0.04rad = -2.29deg\end{aligned}$$

To calculate the tail-created lift coefficient, the lifting line theory is employed. MATLAB code is utilized to calculate the tail lift coefficient with an angle of attack of 2.29 deg. The tail is expected to generate a C_{L_h} of 0.121, but it generates a C_{L_h} of 2.3. To increase the tail lift coefficient to the desired value, we need to increase the tail angle of attack. With trial and error and using the same m-file, we find that the tail angle of attack of 1.8 deg generates the desired tail lift coefficient.

$$\alpha_{th} = -1.29deg$$

we need to take into account the downwash.

$$\begin{aligned}\epsilon_o &= \frac{2C_{Lw}}{\pi AR} \\ &= \frac{2 * 0.6}{\pi * 7.8} = 0.048rad \\ \frac{\partial \epsilon}{\partial \alpha} &= \frac{2C_{L_{\alpha w}}}{\pi AR} = \frac{2 * 6.8}{\pi 7.8} = 0.55rad\end{aligned}$$

STABILITY ANALYSIS

$$C_{m_\alpha} = C_{L_{\alpha wf}}(h - h_0) - C_{L_{\alpha h}}\eta_h \frac{S_h}{S} \left(\frac{l}{MAC} - h \right) \left(1 - \frac{\partial \epsilon}{\partial \alpha} \right)$$

Putting in our values we get,

$$C_{m\alpha} = -1.611/rad$$

Tail Design Data		
SNo.	Parameter	Value
1	L_{HT}	3.32
2	L_{VT}	3.87m
3	Tail Volume Coefficient (V_{HT})	0.65
4	Fin Volume Coefficient (V_{VT})	0.04
5	Horizontal Tail Area(S_{HT})	3.2m ²
6	Vertical Tail Area(S_{VT})	1.54m ²
7	Horizontal Tail AR (AR_{HT})	5.2
8	Span (b_{HT})	4.05m
9	Span (b_{VT})	2.42m
10	λ_{HT}	0.5
11	λ_{VT}	0.5
12	($C_{r_{HT}}$)	1.00m
13	($C_{t_{HT}}$)	0.50m
14	($C_{r_{VT}}$)	1.2mm
15	($C_{t_{VT}}$)	0.75m
16	($C_{MAC_{HT}}$)	0.78m
17	($C_{MAC_{VT}}$)	0.8m
18	Dihedral angle (Γ_T)	0deg
19	Sweep angle HT ($\lambda_{c/4HT}$)	45deg
20	Sweep angle VT ($\lambda_{c/4VT}$)	34deg
21	Airfoil	NACA 0009

Table 10: Values of all parameters of the tail design

8 Rotor Selection and Performance

The peak thrust-to-weight ratio must be 1.39[10]. Based on this we have done calculations for disc loading and peak power for 6-12 vertical propeller configurations. The best configuration seems to be 12 propeller configuration. The overall mass and power requirements seem to be reasonable for this configuration.

For hovering flight, the performance prediction of a rotor blade is made with the help of Blade Element Momentum Theory (BEMT) by writing a computer program on MATLAB, which gives us the required thrust and power generated by the given rotor and RPM. The blade element momentum theory for hovering rotors is a hybrid method that combines the basic prin-

VTOL Propellers					
peak T/W	1.39	1.39	1.39	1.39	1.39
Weight(MTOW)	15780	15780	15780	15780	15780
Peak Thrust(N)	21934.2	21934.2	21934.2	21934.2	21934.2
Number of propellers	12	10	8	6	4
Wingchord length	10	10	10	10	10
MAX Cover available for propellers	9	9	9	9	9
Max Diameter(m)	1.5	1.8	2.25	3	4.5
peak thrust per propeller	1827.85	2193.42	2741.775	3655.7	5483.55
Disc Loading	1034.87615	862.3967917	689.9174334	517.438075	344.9587167
FOM	0.7	0.7	0.7	0.7	0.7
power loading	0.03405939216	0.03731019476	0.04171406587	0.04816725432	0.0589925977
power per propeller	53666.54787	58788.75771	65727.82928	75895.95985	92953.18759
Power per propeller(KW)	53.66654787	58.78875771	65.72782928	75.89595985	92.95318759
TOTAL power (KW)	643.9985745	587.8875771	525.8226342	455.3757591	371.8127503
VTOL time(min)	15	15	15	15	15
Energy(J)	48299893.09	52909881.94	59155046.35	68306363.87	83657868.83
Total energy approx(KJ)	579598.717	529098.8194	473240.3708	409838.1832	334631.4753
TOTAL energy approx(KW hr) in VTOL phase	160.9997724	146.9720118	131.4557637	113.8440309	92.95326195
MAX Motor Weight per propeller	10.5	10.5	23	23	23
Total Motor Weight	126	105	184	138	92
Percent of TOTAL Weight	7.984790875	6.653992395	11.66032953	8.745247148	5.830164766
Propeller Weight	2.64325	2.746078	2.94105625	3.37465	4.6492
TOTAL propeller weight	31.719	27.46078	23.52845	20.2479	18.5968
Propeller + Motor %	9.99486692	8.394219265	13.15135932	10.02838403	7.008669202

Figure 31: Calculations for all possible VTOL propellers

Radius(m)	0.65
Chord(m)	0.06
Number of Blades	2
Pitch Angle	8 degrees
Solidity	0.088
Thrust(N)	1416
Power(KW)	52.39

Figure 32: Geometric Characteristics for fixed pitch propeller for Vertical Lift

ciples from both blade element and momentum theory approaches. For required thrust, the following rotor characteristics are obtained.

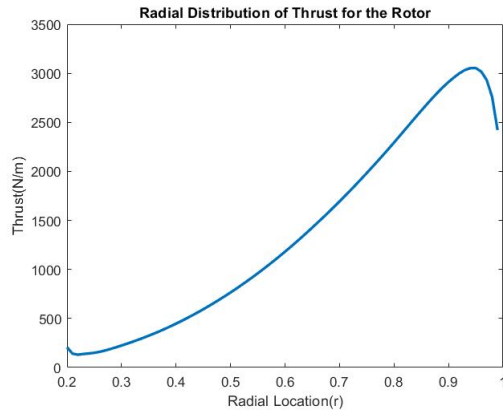


Figure 33: Thrust distribution over the rotor blade

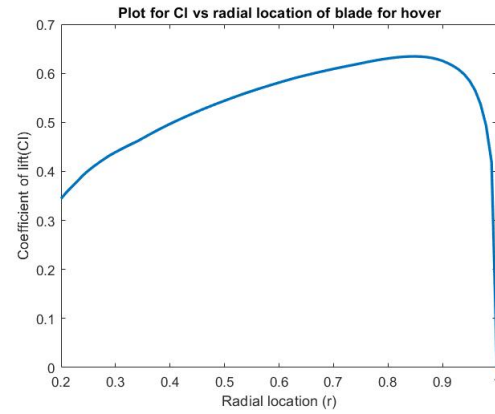


Figure 34: Lift distribution over the rotor blade

Forward Flight Propeller	
Forward Flight Power(KW)	195.1
Total Efficiency of Power elctronics and propeller	0.75
Cruise Speed	58.8
Thrust(N)	2488.520408
Forward Flight time(min)	45
Energy Req(J)	526770000
Energy req(KJ)	526770
Energy(kw/h)	146.3251171

Figure 35: Calculations for Forward flight propeller

9 Powertrain Design

9.1 Introduction

The powertrain of a vehicle refers to the system responsible for generating and delivering power to the wheels. It has many parts, such as the engine, transmission, driveshaft, and axle. Its job is to turn the energy in fuel, batteries, or any other energy source into the mechanical energy needed to move the vehicle.

In hybrid electric vehicles, both internal combustion engines and electric motors make up the powertrain. The combination of these two power sources is better than traditional vehicles in many ways, like using less gas, going faster, and putting out less pollution.

An electric vertical takeoff and landing (eVTOL) aircraft's powertrain is very important because it has to meet specific flight requirements, such as weight limits, power density, and reliability. The choice of powertrain technology can have a big effect on how well, efficiently, and safely the plane works as a whole.

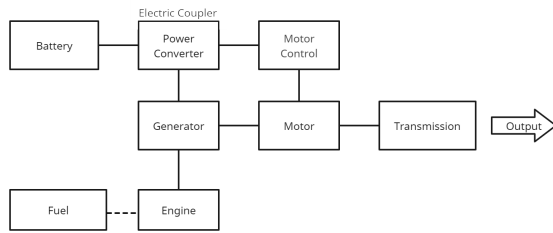


Figure 36: Series Hybrid drive train

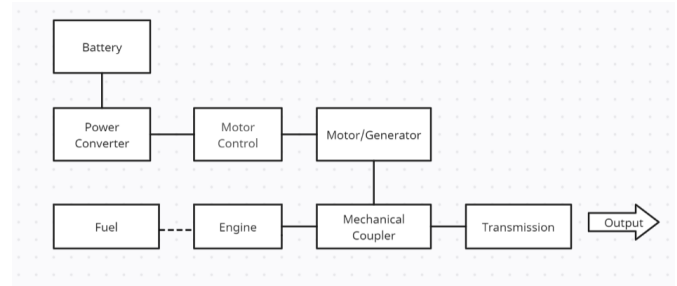


Figure 37: Parallel Hybrid drive train

9.2 Types of Hybrid Systems[9]

1. **Series Hybrid:** A serial hybrid powertrain is one which used a battery pack and a secondary fuel source in a series combination to power the system. This system is also referred to as an "electrical coupling" system. There is a power converter that is responsible for the energy flow within the system i.e., between the battery, secondary fuel source, and the motor.
2. **Parallel Hybrid:** It is a parallel connection of the same elements and is connected via a mechanical coupler referring to the system as "mechanical coupling" system. Using the mechanical coupler, the system can run in either a single mode (the engine alone or the motor alone) or dual mode (the engine and the motor together).
3. **Series-Parallel Hybrid:** As the name suggests, it consists of both mechanical and electrical couplers and can be used in different combinations as the aforementioned systems. The main benefit of this setup is that it is easy to change the configuration while it is in its operating phase. It is also the most common architecture in hybrid vehicles but as it can be clearly seen that it has a major drawback i.e. this architecture makes it hard to control and figure out how much something weighs.
4. **Fuel-Cell Hybrid:** A fuel cell hybrid power system combines a fuel cell system with a battery or internal combustion engine (ICE). Hydrogen fuels the fuel cell system, which electrochemically converts it into electricity. The secondary energy source provides power and energy storage. The fuel cell system is the primary energy source in a fuel cell hybrid, while the secondary energy source provides additional power and stores excess energy. This can improve efficiency, range, and emissions over internal combustion engines.

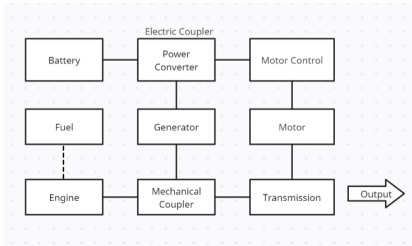


Figure 38: Series-Parallel Hybrid drive train

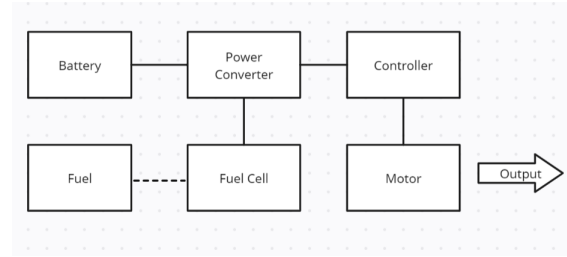


Figure 39: Fuel cell hybrid electric drive train

9.3 Which Hybrid System to choose?

Situations call for certain combinations of hybrid systems, and the ones that are used most often are series hybrid and parallel hybrid combinations. The main benefit of a series configuration is that the energy sources are not tied together. This means that the engine can run on its own and at its most efficient, but it has a major drawback in that the electric motor has to provide all of the propulsion power by itself. This means that it has to be designed for the most power, which makes the drivetrain heavier. We mainly consider series combinations when we need high torque and low speed. On the other hand, the parallel hybrid type saves weight because the machines can be the right size because the power to move forward comes from both subsystems. This results in significant weight loss. Also, the mechanical connection, which is of the parallel type, adds to the complexity.

Still, the most important thing to think about when designing an aircraft is the total weight of the plane when the payload is known. This needs to be optimized using iterative methods because it includes the weight of the fuel and the weight of the batteries, which change when the powertrain system is being designed.

9.4 Design[8]

Since we have already known the wing loading and the different parameters required to get the power we need for the aircraft to take off, we will now shift towards the selection and design of the powertrain system.

From the synopsis report, we did come to the conclusion that our aircraft design type will be a lift-and-cruise type consisting of 12 propellers. Since each propeller will be powered by its own motor, we need to figure out how much the motor needs to weigh

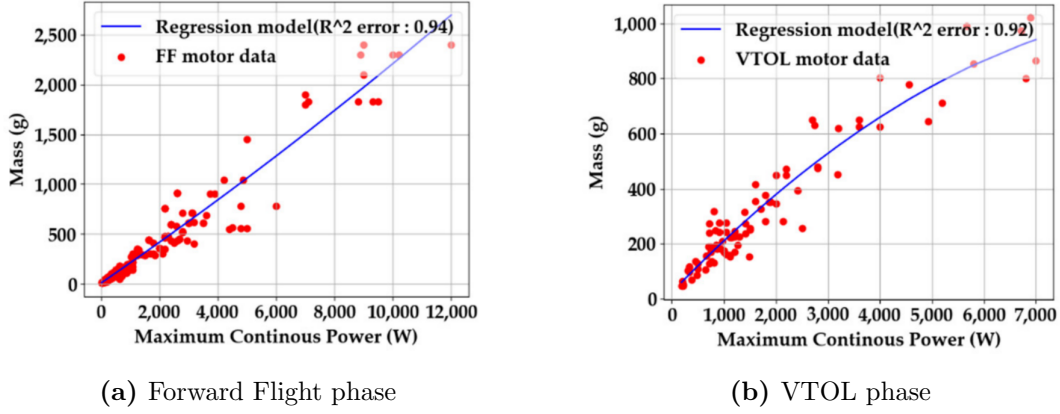


Figure 40: Regression data for different phases of flight

in order to power the propeller and create the necessary amount of vertical thrust. Same applies for the forward flight case where the forward propeller is driven by a separate motor and has a different power requirement so the sizing is done separately. Last but not the least, separate design considerations are to be carried out for the energy sources in different phases of flight operation i.e., batteries for VTOL phase and fuel cell for forward flight phase.

9.5 Motor Sizing[8]

For two different parts of the rescue operation, the motor size needs to be set separately. In this case, there are two phases: Vertical liftoff (or VTOL) and forward flight (or FF). Due to the differences in power requirements between the two phases of the operation, a dual situation is necessary. There will be a difference in the mass of the motors during the VTOL phase as compared with the FF phase.

So, different regression models are made with data points that are more cluttered near the amount of continuous power needed by the respective motor. To make the regression model, we plotted the mass against the continuous power needed by the motor, which we got from the propeller power loading. We get the equations for the VTOL and FF phases, respectively, as follows:

$$M_{mot.VTOL} = 0.922 \times 10^{-5} P_{max.VTOL}^2 + 0.196 P_{max.VTOL} + 23.342$$

$$M_{mot.FF} = 0.196 \times 10^{-5} P_{max.FF}^2 + 0.201 P_{max.FF} + 5.772$$

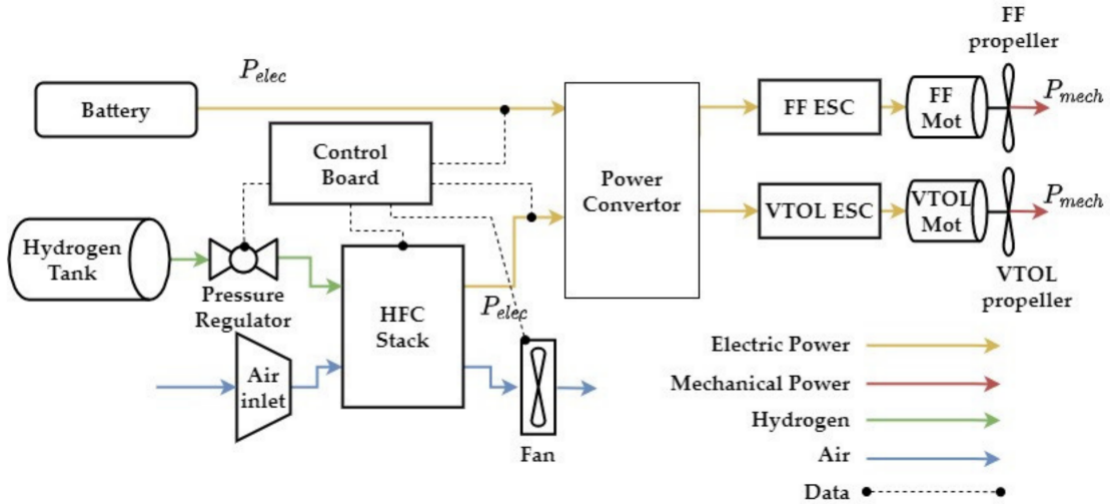


Figure 41: Hydrogen Fuel Cell eVTOL hybrid concept

Here, "electrical power" means "maximum power," and it is a value that takes into account the motor's efficiency based on the mechanical power calculated through power loading. Also, the motor's efficiency is usually taken to be between 90 and 95 percent.

9.6 Cell Selection

A battery is a particular combination of cells. We need to design the battery so that it can give the propellers the power they need. You can't just pick a battery off the shelf because the design of a battery takes into account things like its weight, energy density, volume, nominal voltage, current rating, and what it will be used for. For example, we can't use the battery in our homes as a power source in our airplanes because it has a lot of weight, which would not be the best solution. We also can't just buy any battery off the shelf because they are designed based on the application.

Based on how much power each propeller needs, we can figure out that each one needs a certain amount of voltage and current to generate the power it needs to turn.

Below is the tabulated data for three different voltage and current ratings, which have been illustrated in the table below. The process of putting together batteries is looked at for different types of cells made by different companies. The total weight of the battery is then calculated accordingly. We perform these steps in three different situations: when one battery powers all twelve propellers, when six batteries power all twelve propellers, or when one battery powers one propeller each. We put this information in three

Required Voltage by each motor(V)	580	390	140
Required Current per motor(A)	89.65514	133.34	371.42857
Total Current(A)	1075.8621	1600	4457.142857
Current Required by 2 motors	179.31028	266.68	742.85714

Figure 42: Different voltage and current data

Cell	Sony US18650V3	Samsung INR18650-35E	A123 Systems ANR26650M1B	Murata LVP123035	A123 Systems ANR26650M1B	
Nominal Voltage(V)	3.6	3.6	3.3	3.7	3.3	
Nominal Current(A)	10	15	20	10	70	
Weight(gm)	46	48	62	44	76	
No. of cells in series connection	161.1111111	161.111	175.7575	156.7567568	175.7575758	
No. of parallel connection	107.58621	71.72414	53.7931	107.58621	15.36945857	580 V
Weight of the battery	797.3333563	554.6663	586.1816	742.0540755	205.2987072	
No. of cells in series connection	108.333	108.333	118.1818	105.4054	118.1818182	
No. of parallel connection	160	106.666	80	160	22.85714286	390 V
Weight of the battery	797.331	554.6615	586.1817	742.054	205.2987013	
No. of cells in series connection	38.888	38.888	42.4242	37.8378	42.42424242	
No. of parallel connection	445.714	297.143	222.8271	445.714	63.67346939	140 V
Weight of the battery	797.314	554.654	586.1022	742.053	205.2987013	
No. of cells in series connection	161.1111111	161.111	175.7575	156.7567568	175.7575758	
No. of parallel connection	8.965514	5.977	4.4827	8.965514	1.280787714	580 V
Weight of a battery	66.44442042	46.2221	48.8484	61.83781548	17.10821892	
Total weight of battery	797.3330451	554.665	586.1813	742.0537858	205.2986271	

Figure 43: Estimation of Battery weight assuming single battery

tables, and from these tables, we can see that the total weight of the batteries is the same no matter how many are used, as long as the nominal voltage and nominal current of the cells stay the same.

9.6.1 Sample Calculation

Let's consider the following data:

The voltage required by each motor = 580 V

Current required by each motor = 89.65514 A

Cell	Sony US18650V3	Samsung INR18650-35E	A123 Systems ANR26650M1B	Murata LVP123035	A123 Systems ANR26650M1B	
Nominal Voltage(V)	3.6	3.6	3.3	3.7	3.3	
Nominal Current(A)	10	15	20	10	70	
Weight(gm)	46	48	62	44	76	
No. of cells in series connection	161.1111	161.111	175.7575	156.7567568	175.7575	
No. of parallel connection	17.931028	11.954	8.9655	17.931028	2.5616	580 V
Weight of a battery	132.888	92.444	97.6967	123.6756	34.2164	
Total weight of battery	797.332	554.665	586.1804	742.05378	205.2985	
No. of cells in series connection	108.333	108.333	118.1818	105.4054	118.1818182	
No. of parallel connection	26.668	17.7786	13.334	26.668	3.8097	390 V
Weight of a battery	132.895	92.4484	97.7018	123.6818	34.218	
Total weight of battery	797.3707	554.6906	586.211	742.0908	205.3082	
No. of cells in series connection	38.888	38.888	42.4242	37.8378	38.888	
No. of parallel connection	74.2856	49.5238	37.1428	74.2856	10.61224	140 V
Weight of a battery	132.8856	92.4422	97.6968	123.6754	31.36436	
Total weight of battery	797.314	554.6539	586.1812	742.0521	188.18617	

Figure 44: Estimation of Battery weight assuming 6 battery

Cell	Sony US18650V3	Samsung INR18650-35E	A123 Systems ANR26650M1B	Murata LVP123035	A123 Systems ANR26650M1B	
Nominal Voltage(V)	3.6	3.6	3.3	3.7	3.3	
Nominal Current(A)	10	15	20	10	70	
Weight(gm)	46	48	62	44	76	
No. of cells in series connection	161.1111111	161.111	175.7575	156.7567568	175.7575758	580 V
No. of parallel connection	8.965514	5.977	4.4827	8.965514	1.280787714	
Weight of a battery	66.44442042	46.2221	48.8484	61.83781548	17.10821892	
Total weight of battery	797.3330451	554.665	586.1813	742.0537858	205.2986271	
No. of cells in series connection	108.333	108.333	118.1818	105.4054	118.1818182	390 V
No. of parallel connection	13.334	8.8893	6.667	13.334	1.904857143	
Weight of a battery	66.4475	46.2242	48.8509	61.8409	17.10908052	
Total weight of battery	797.3707	554.6906	586.211	742.0908	205.3089662	
No. of cells in series connection	38.888	38.888	42.4242	37.8378	38.88888889	140 V
No. of parallel connection	37.1428	24.7619	18.5714	37.1428	5.306122429	
Weight of a battery	66.4428	46.2211	48.8484	61.8377	15.68253962	
Total weight of battery	797.314	554.6539	586.1812	742.0521	188.1904755	

Figure 45: Estimation of Battery weight assuming 12 battery

The total current required by all the motors = $89.65514 \times 12 = 1075.8621$ A

Suppose we take the cell to be a “**Sony US18650V3**” with the following specifications:

Nominal Voltage = 3.6 V

Nominal current = 10 A

Weight = 46 gm

Now,

For the number of series connections, calculations were performed on nominal voltages as follows:

Nominal voltage of battery pack/Nominal voltage of cell

The number of parallel cells is calculated using the current criteria as follows:

Max Current required from battery pack/Maximum continuous current of the cell

Therefore here, for the number of series connections = $580/3.6 = 161.11111$

For the number of parallel connections = $1075.8621/10 = 107.58621$

Hence, the weight of battery = $(161.1111 \times 107.58621 \times 46)/1000 = 798$ kg

9.6.2 Result[4]

Based on the three sets of tabulated data, we conclude that the cell “**A123 Systems ANR26650M1B**” is most feasible for designing the battery since it contributes the least weight. We get nearly 189 kg when we use 140 volts as the voltage. Here, we get nearly 189 kg when we use 140 volts as the voltage.

9.7 Fuel Cell as a Secondary source of energy![5]

Because the Air Ambulance is a hybrid, the energy needs during the VTOL phase are met by the battery system. Secondary energy sources are responsible for energy demand during forward flight. As a result, we chose the **”fuel cell”** for this phase. Fuel cells can offer several advantages as a secondary energy source in a hybrid type aircraft compared to traditional internal combustion engines (ICEs) or batteries. Some of the key advantages are:

- **High energy efficiency:** Fuel cells are very good at turning hydrogen into electricity. They can do this with an efficiency of up to 60%. This is better than traditional ICEs, which usually only work 30–40% of the time.
- **Clean and quiet operation:** Fuel cells produce water as the only byproduct of their reaction, resulting in much lower emissions compared to traditional ICEs. Additionally, fuel cells operate quietly, reducing the noise pollution generated by traditional ICEs.
- **Increased range and endurance:** Fuel cells have a higher energy density compared to batteries, meaning they can store more energy in a smaller and lighter package. This can increase the range and endurance of a hybrid aircraft compared to a purely battery-powered vehicle.
- **Improved safety:** Fuel cells are safer than traditional ICEs as they do not have a high-temperature combustion process, reducing the risk of fire. Additionally, hydrogen is a non-toxic gas, reducing the risk of harm in the event of a leak.

9.7.1 Fuel Cell Design

As per the mission requirements, the requirements of fuel cell for powering the forward propeller are:

Fuel Cell/Propeller Requirements	
Forward Flight Power(KW)	195.1
Forward Flight Time(min)	45
Energy Required(KJ)	526770
Energy(KW/Hr)	146.3251171

Since we can see that the power required is nearly 200KW, hence we need a fuel cell which can fulfill the needs. Below is the tabulated data for some of the fuel cells which can be used in this mission.

Data for fuel cells available in the market[6]		
Fuel Cell	Power Output(KW)	Weight(Kg)
FCGen-HPS Fuel Cell System by Hydrogenics	195	60
Symbio FC5 Fuel Cell System by Symbio FC	200	45
Proton OnSite M-series Fuel Cell System	200	45
Nel Hydrogen Fuel Cell System	200	40
H-Gen Fuel Cell System by Symbio	195	60

In the above tabulated data, we have given the dry weight of the fuel cell, which is its weight when there is no fuel present. Since hydrogen has a very high energy density as compared to petrol or diesel, a very small quantity can supply ample energy without significantly increasing the weight.

9.8 Volume occupied by Battery set and Fuel cell

9.8.1 Battery

Since we already know that the number of batteries doesn't make a big difference in how much power the propellers need, we will only use one battery to power all of the propellers to save space. In addition, we determined the cell used to construct the battery was "**A123 Systems ANR26650M1B.**" The physical dimensions (in mm) of this cell are: Ø26 x 65.

Hence the volume of a single is around $3.451 \times 10^{-5} m^3$.

Therefore the net volume occupied by all the cells in nearly cuboidal arrangement will be:

$$\begin{aligned}
 &= \text{No. of cells in series connection} \times \text{No. of parallel connection} \times \text{Vol. of a single cell} \\
 &= 38.888 \times 10.61224 \times 3.451 \times 10^{-5} \\
 &= 0.0142419 m^3
 \end{aligned}$$

$$= 14.2419 \text{ L}$$

As cells are cylindrical in shape, this is not the actual volume, and the casing and wiring system will also occupy some space. In light of all these factors, we can conclude that the battery will nearly occupy a volume of 20 L, which is a quite small volume.

9.8.2 Fuel Cell[7]

We had already selected our fuel cell for the mission. Now we need to figure out roughly how much space it would take up on the plane. Let's choose **"FCGen-HPS Fuel Cell System by Hydrogenics"** and proceed accordingly. Its dimensions are 484 x 555 x 195 (in mm), which can be found on the company's website. So, it is easy to figure out how big it is. Its volume comes out to be 0.0523809 m^3 , which is just about 53 liters.

10 Fuselage Design

10.1 Introduction

The primary function of the fuselage is to accommodate the payload. The fuselage is designed according to the given requirements, with a given volume of 9 m^3 accommodating one paramedic, one patient, and the required equipment for emergency treatment. All these items to be accommodated in the fuselage need a proper internal arrangement and enough space is required for the free movement of the paramedic. The points kept in mind while designing the internal arrangement are:

1. Keep the fuselage as small and compact as possible
2. Arrangement to be symmetric from the top view as far as possible
3. There must be sufficient space to accommodate all of the items
4. Usable loads such as fuel must be close to the aircraft's center of gravity
5. Arrangements must be such that the aircraft's center of gravity is close to the wing/fuselage aerodynamic center

Fuselage Max Width	2.35 m
Fuselage Max Length	4.71m
Cabin Max Length	2.79 m
Cabin Max Width	1m
Cabin Max Height	2.06m

Table 11: Specifications of Fuselage

10.2 Dimensions

10.3 Ergonomics

The field of human factors engineering uses scientific knowledge about human behavior in specifying the design and use of a human/machine system. The aim is to improve system efficiency by minimizing human error and optimize performance, comfort, and safety. Proper ergonomic design is necessary to prevent repetitive strain injuries, which can develop over time and can lead to long-term disability.

Since, the weight reduction factor come into picture, we cant make an air ambulance as comfortable as a road ambulanca vehicle, it will seem to much more compact and almost all corners will be utilized in order to make up space for storage or reduce the overall weight of the vehicle.

- The size of an average male patient is more than the average female patient, thus the stretcher is made for the larger size thus inculcating the small size patients also, the tolerance is also taken, and the length of the bed is taken to be 1.8m
- The paramedic will have to crouch many times in the air ambulance if one wishes to use the sink, as it is on the far end of the cabin whose shape has been modified in order to maintain a streamlined aerodynamic shape.

10.4 Cabin Design

The ambulance will not accommodate the cockpit, since the design is autonomous. Other than that, the cabin needs to accommodate all medical equipment namely:-

- Seat
- Stretcher
- Monitor

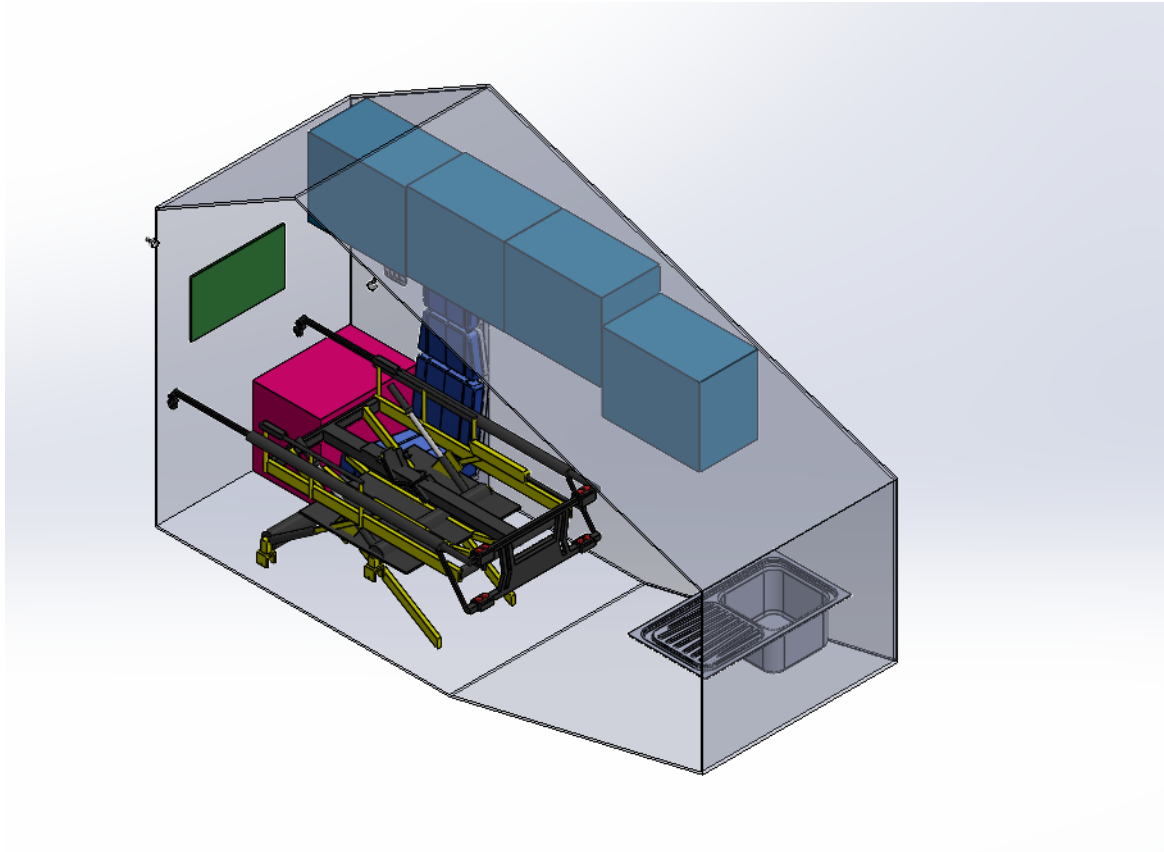


Figure 46: Isometric view of the complete cabin CAD assembly

- Storage Cabinets (2)
- Sink for washing
- Transport Ventilator
- ECG System
- Emergency Bags and Boxes (3)
- Bleed Control and Trauma Kit (5)
- Burns Kit (5)
- Defibrillators (2)
- Injection and Infusion Kits (5)
- The blue cabinets are well within reach of the paramedic and host all the kits required to treat the patient. Their sizes have been estimated from the cumulation of all the equipment mentioned in the guidelines.

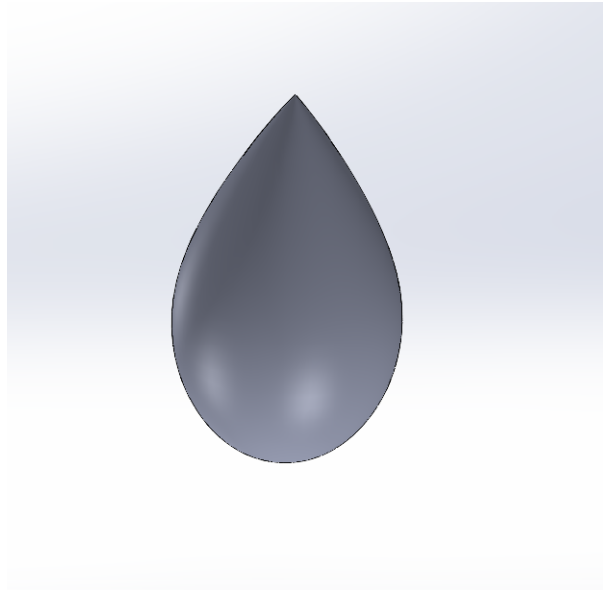


Figure 47: First Iteration: Side view of basic teardrop shape

- The pink cabinets host three D-7 oxygen tanks of 17 inches and are again well within the reach of the paramedic's accessible volume.
- Lights are provided in the cabin and the switches can be manipulated with just the stretch of one's arm.
- The medical monitor is placed facing the paramedic so that monitoring the patients' vitals is easier.

10.5 Outer Skin Design

After accommodation of the cabin, fuel tanks, and others, we move on to the secondary motive of the fuselage, to be aerodynamic and produce minimum drag.

The most aerodynamic shape in nature is considered to be a teardrop, the initial shape is that of a teardrop, and afterward iterations and analysis on designs we arrive at the final design which inculcates all components as aerodynamic.

10.5.1 Iterations

The process followed to arrive at the final design:

1. Started from a basic teardrop shape

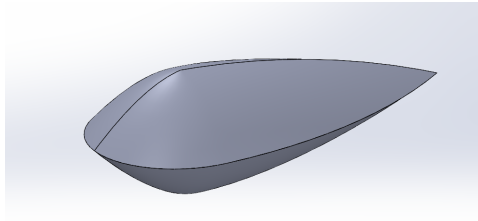


Figure 48: Second Iteration of Outer Skin

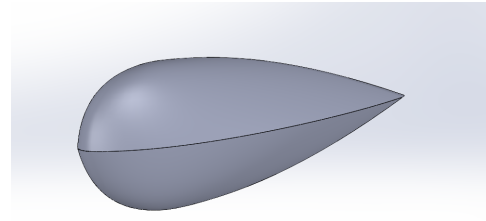


Figure 49: Third Iteration of Outer Skin

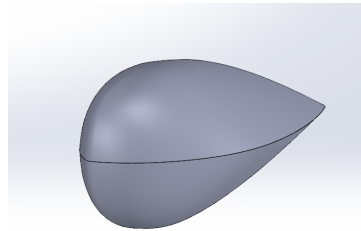


Figure 50: Final Iteration of Outer Skin

2. Second iteration to accommodate a cuboidal cabin, which resulted in edges and less aerodynamic efficiency
3. Final iteration with minor changes

10.6 Accommodation of Cabin in the Fuselage

As one of the main motives of the fuselage is to encapsulate the cabin, the initial design accommodates the cuboidal cabin well. Still, it resulted in a lot of additional weight. Thus, we removed the concept that the cabin had to be cuboidal and made modifications according to the size of the cabin components, cabin and the aerodynamic efficiency of the whole fuselage.

10.7 CFD Analysis

The aerodynamic analysis for all the iterations was done and the final design was finalized as it was the best fit between aerodynamic efficiency and accommodation of all components. For the final aerodynamic shape, the following variation of lift and drag was observed,

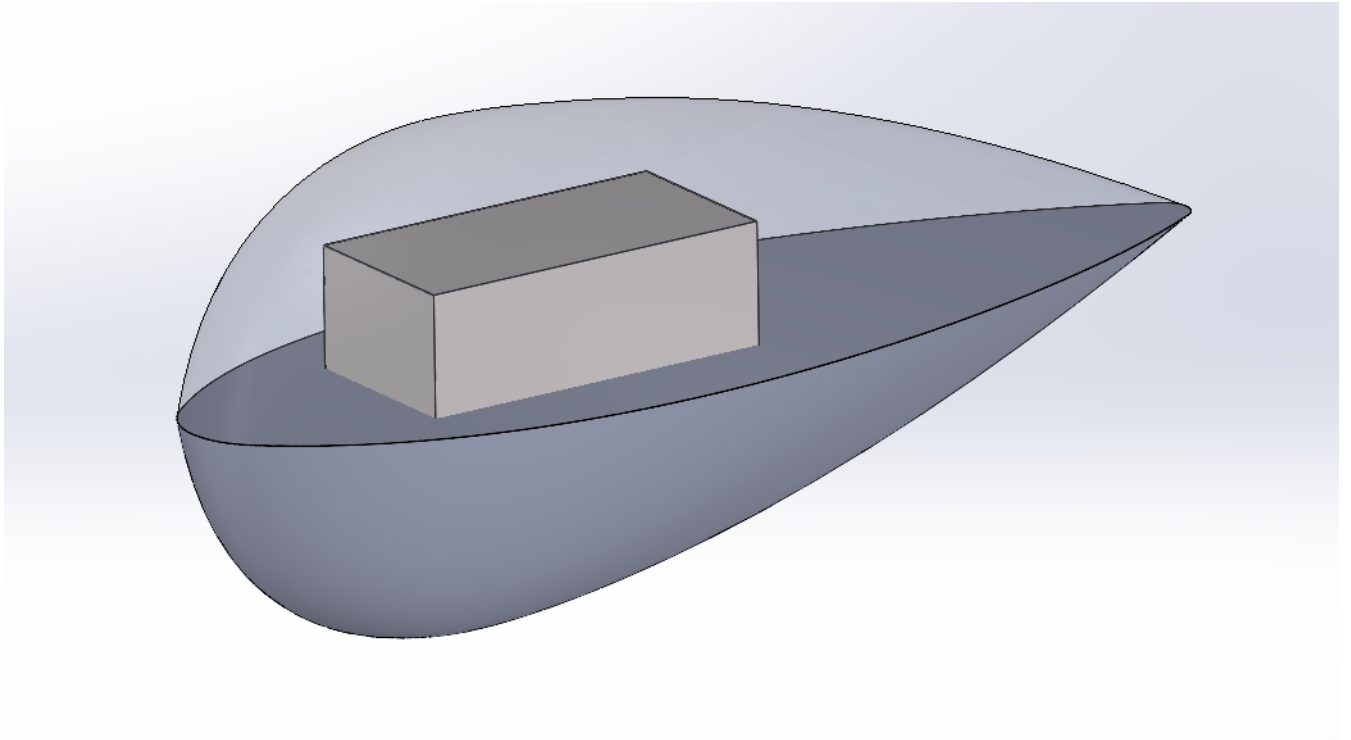


Figure 51: One of the initial iterations of both outer skin and cabin

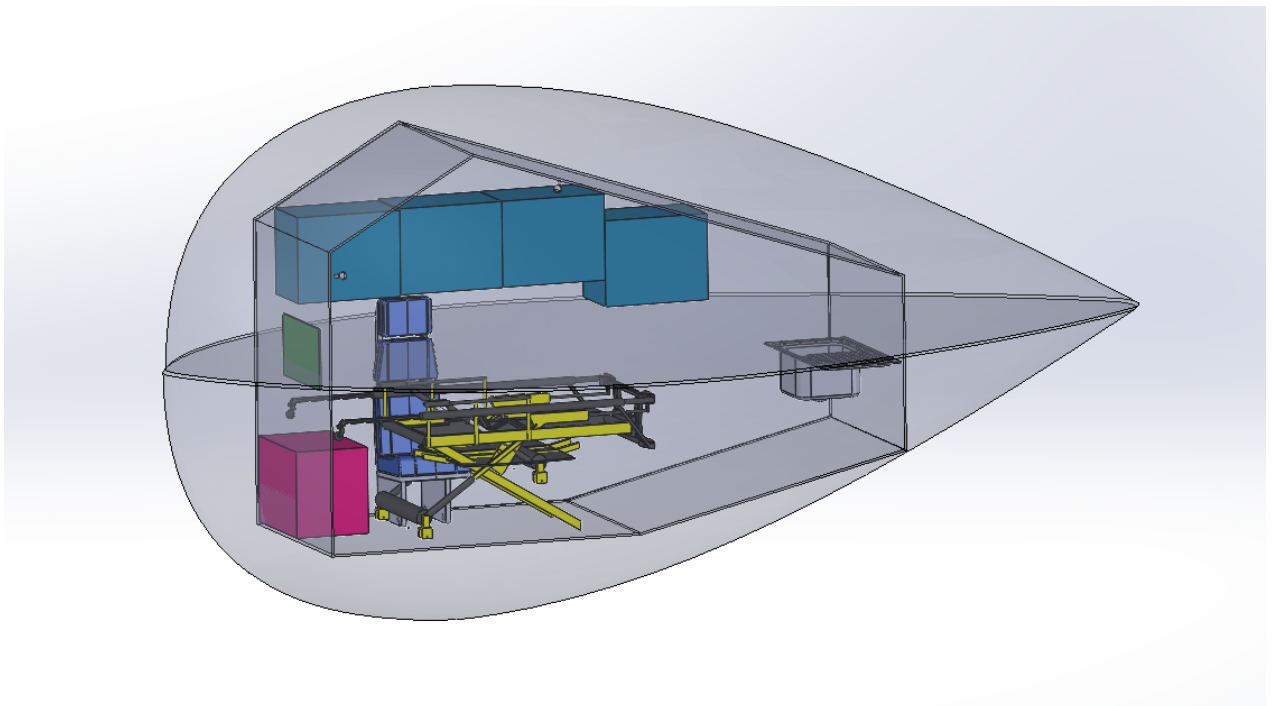


Figure 52: Diametric View of Final Cabin CAD Assembly

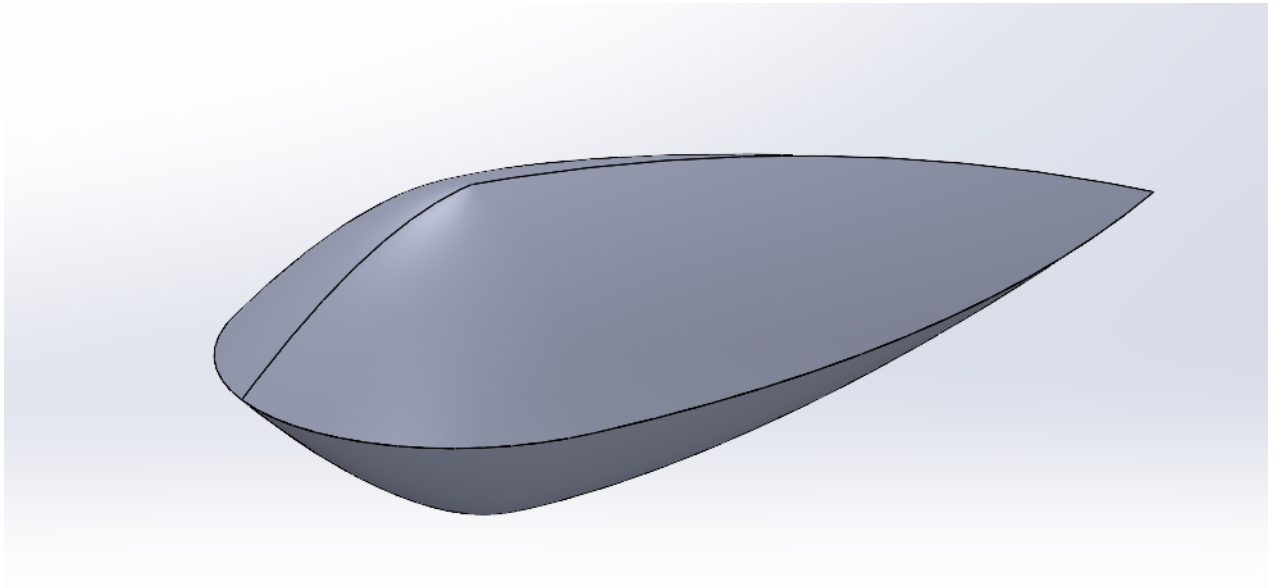


Figure 53: Side View of Final Cabin CAD Assembly

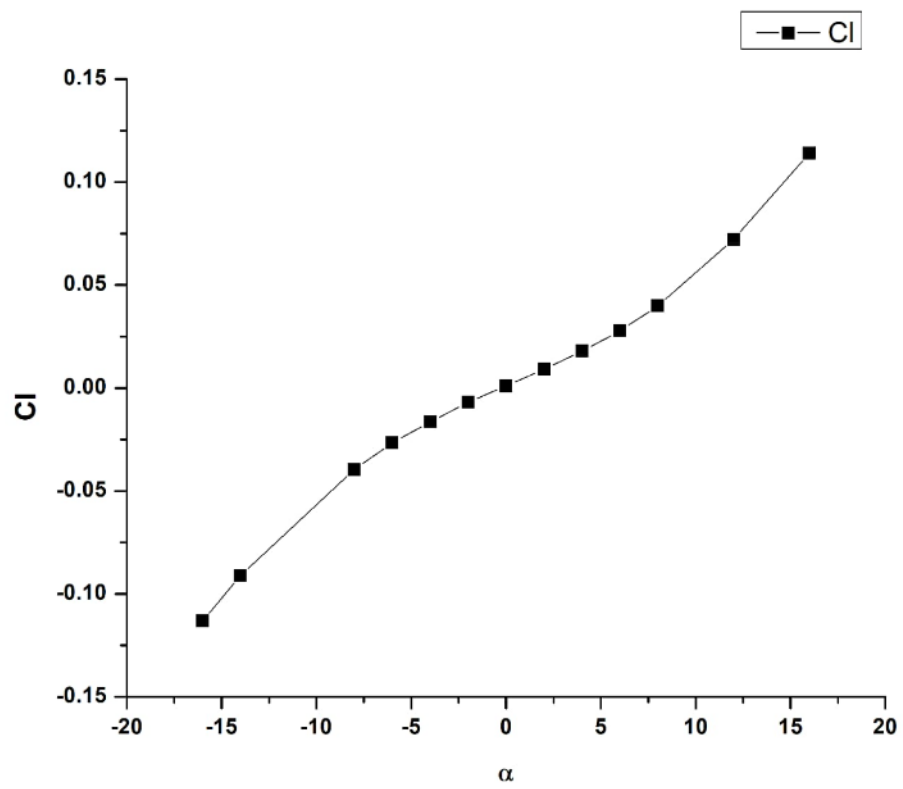


Figure 54: Variation of Lift coefficient with AoA

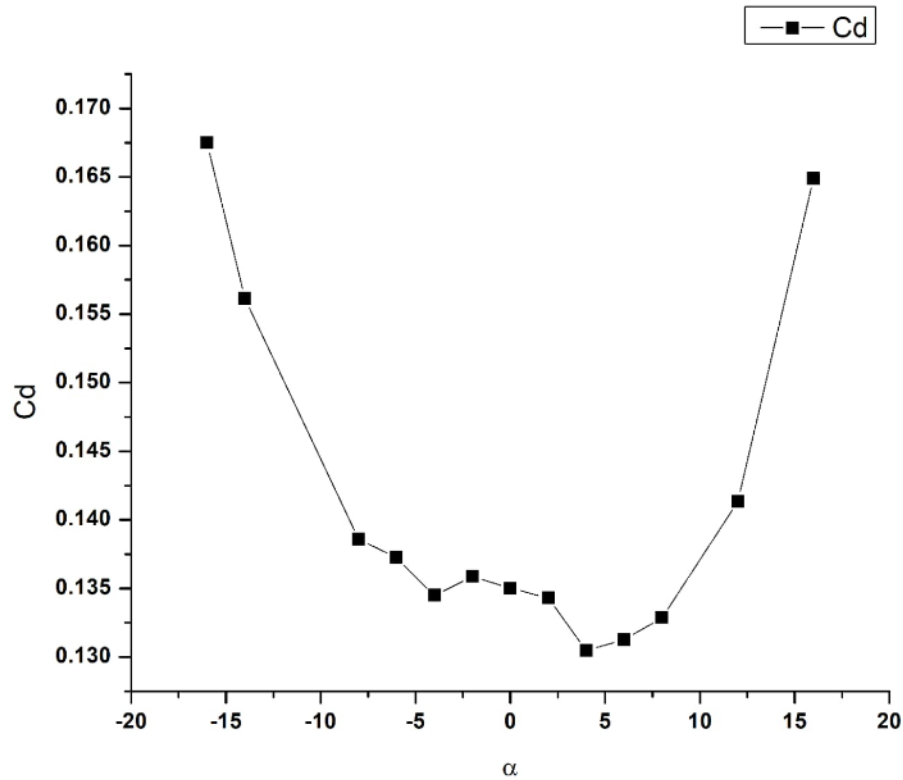


Figure 55: Variation of Drag coefficient with AoA

References

- [1] URL: <https://evtol.news/aircraft>.
- [2] URL: https://maunaloahelicopters.edu/library/Rotorcraft_Training_Manuals/Airbus_Eurocopter_Helicopter/EC_135/EC_135_Technical_Data.pdf.
- [3] URL: https://economictimes.indiatimes.com/helicopters-in-mumbai-fly-half-the-recommended-altitude/articleshow/10563705.cms?utm_source=contentofinterest&utm_medium=text&utm_campaign=cppst.
- [4] URL: <https://www.buya123products.com/goodsdetail.php?i=6>.
- [5] URL: <https://www.twi-global.com/technical-knowledge/faqs/what-are-the-pros-and-cons-of-hydrogen-fuel-cells>.
- [6] URL: <https://chat.openai.com>.
- [7] URL: https://www.ballard.com/docs/default-source/spec-sheets/fcgen-hps.pdf?sfvrsn=704ddd80_4.

- [8] Jae-Hyun An et al. “Advanced Sizing Methodology for a Multi-Mode eVTOL UAV Powered by a Hydrogen Fuel Cell and Battery”. In: *Aerospace* 9.2 (2022). ISSN: 2226-4310. DOI: 10.3390/aerospace9020071. URL: <https://www.mdpi.com/2226-4310/9/2/71>.
- [9] Junghsen Lieh et al. “Design of Hybrid Propulsion Systems for Unmanned Aerial Vehicles”. In: July 2011. ISBN: 978-1-60086-949-5. DOI: 10.2514/6.2011-6146.
- [10] Daniel P Raymer. *Aircraft design: A conceptual approach*. 4. ed. AIAA education series. Reston, Va.: American Institute of Aeronautics and Astronautics, 2006. ISBN: 1563478293. URL: <http://www.loc.gov/catdir/toc/ecip068/2006004706.html>.